

Progress of the TianQin project

Jun Luo¹, Shaojun Bai⁴, Yan-Zheng Bai², Lin Cai², Hao Dang⁵, Qijia Dong⁶, Hui-Zong Duan¹, Yuanbo Du¹, Lei Fan¹, Xinju Fu⁷, Yong Gao⁷, Xingyu Gou⁷, Defeng Gu^{1,8}, Changlei Guo¹, Wei Hong², Bin Hu⁴, Heran Hu⁷, Ming Hu², Yi-Ming Hu¹, Fa Peng Huang¹, Xin Ji⁹, Yuan-Ze Jiang², En-Kun Li¹, Hongyin Li¹, Ming Li¹, Ming Li³, Yong Li⁷, Zhu Li¹, Zizheng Li¹, JunXiang Lian¹, Yu-Rong Liang², Xudong Lin¹, Jianping Liu¹, Lin-Xia Liu¹, Kui Liu¹, Li Liu², Minghe Liu³, Qi Liu¹, Yan-Chong Liu², Yue Liu³, Peng-Shun Luo², Yingxin Luo¹, Yi-Qiu Ma², Yun Ma², Yunhe Meng^{1,8}, Vadim Milyukov¹⁰, Jian-Guo Peng², Konstantin Postnov¹⁰, Shao-Bo Qu², Tilei Shan³, Cheng-Gang Shao², Changfu Shi¹, Pei-Yi Song², Yunfei Song⁵, Wei Su¹, Ding Yin Tan¹, Shuping Tan⁷, Yu-Jie Tan², Wenhai Tan¹, Liangcheng Tu¹, Cheng-Rui Wang², Guoyong Wang⁹, Lijiao Wang⁷, Pan-Pan Wang², Shun Wang², Xiaoyong Wang⁴, Xudong Wang⁷, Yan Wang², Ran Wei⁵, Shu-Chao Wu², Jie Xu¹, Zhi-Lin Xu², Chao Xue¹, Hao Yan², Yong Yan¹, Changpeng Yang⁵, Shanqing Yang¹, Hsien-Chi Yeh^{1†}, Hang Yin², Yelong Tong⁵, Jian-Bo Yu², Wen-Hao Yuan², Bu-Tian Zhang², Dexuan Zhang¹, Jian-dong Zhang¹, Jie Zhang², Lihua Zhang³, Xuefeng Zhang^{1‡}, Guoying Zhao¹, Liqian Zhao⁶, Xin Zhao⁵, An-Nan Zhou², Hao Zhou², Peng Zhou¹, Yupeng Zhou⁵, Ze-Bing Zhou^{2‡}, Fan Zhu¹, Liang-Gui Zhu¹¹, Lin Zhu², Kui Zou⁷, Jianwei Mei^{1*}

¹MOE Key Laboratory of TianQin Mission, TianQin Research Center for Gravitational Physics & School of Physics and Astronomy, Frontiers Science Center for TianQin, Gravitational Wave Research Center of CNSA, Sun Yat-sen University (Zhuhai Campus), Zhuhai 519082, China

²National Gravitation Laboratory, MOE Key Laboratory of Fundamental Physical Quantities Measurement, and School of Physics, Huazhong University of Science and Technology, Wuhan 430074, China

³DFH Satellite Co., Ltd., Beijing 100094, China

⁴Beijing Institute of Space Mechanics & Electricity, Beijing 100076, China

⁵National Key Laboratory of Spacecraft Thermal Control of Institute of Spacecraft System Engineering, Beijing 100094, China

⁶Space Star Technology CO., LTD., Beijing 100095, China

⁷Beijing Institute of Control Engineering, Beijing 100094, China

⁸School of Artificial Intelligence, Sun Yat-sen University (Zhuhai Campus), Zhuhai 519082, People's Republic of China

⁹China Academy of Space Technology (Xi'an), Xi'an 710199, Shanxi, China

¹⁰Sternberg Astronomical Institute, M.V. Lomonosov Moscow State University, Moscow 119234, Russia

¹¹Kavli Institute for Astronomy and Astrophysics, Peking University, Beijing 100871, China

E-mail:

*meijw@sysu.edu.cn

†yexianji@mail.sysu.edu.cn

‡zhangxf38@mail.sysu.edu.cn

‡zhouzb@mail.hust.edu.cn

18 February 2025

Abstract. TianQin is a future space-based gravitational wave observatory targeting the frequency window of 10^{-4} Hz \sim 1 Hz. A large variety of gravitational wave sources are expected in this frequency band, including the merger of massive black hole binaries, the inspiral of extreme/intermediate mass ratio systems, stellar-mass black hole binaries, Galactic compact binaries, and so on. TianQin will consist of three Earth orbiting satellites on nearly identical orbits with orbital radii of about 10^5 km. The satellites will form a normal triangle constellation whose plane is nearly perpendicular to the ecliptic plane. The TianQin project has been progressing smoothly following the “0123” technology roadmap. In step “0”, the TianQin laser ranging station has been constructed and it has successfully ranged to all the five retro-reflectors on the Moon. In step “1”, the drag-free control technology has been tested and demonstrated using the TianQin-1 satellite. In step “2”, the inter-satellite laser interferometry technology will be tested using the pair of TianQin-2 satellites. The TianQin-2 mission has been officially approved and the satellites will be launched around 2026. In step “3”, i.e., the TianQin-3 mission, three identical satellites will be launched around 2035 to form the space-based gravitational wave detector, TianQin, and to start gravitational wave detection in space.

Keywords: TianQin, Gravitational wave, Black hole, Inertial reference, Inter-satellite laser interferometry

Contents

1 Introduction 3

2 Science Objectives of TianQin 5

2.1 Astrophysics with TianQin 6

2.1.1 Detection ability of TianQin 6

2.1.2 Stellar physics 7

2.1.3 Birth and growth of massive black holes 8

2.1.4 Environment surrounding massive black holes 8

2.2 Fundamental Physics with TianQin 9

2.2.1 Testing the key predictions of GR 9

2.2.2 Looking for possible signatures of beyond GR effect 11

2.2.3 Environmental effects 12

2.2.4 New fundamental matter and interactions 13

2.3 Cosmology with TianQin 15

2.3.1 Constraining the Λ CDM model 15

2.3.2 Probing the equation of state of dark energy 17

3 Concept and design of TianQin 17

3.1 Special challenges 18

3.2 Orbit and constellation 18

3.3 Space environment 19

3.4 Science payload 20

3.5 Satellite platform 21

3.6 Thermal control 22

4 Developing Key Technologies for TianQin 23

4.1 Inertial reference 23

4.1.1 Inertial sensor 23

4.1.2 Micro-Newton thruster 25

4.1.3 Drag-free control 26

4.2 Intersatellite laser interferometry 27

4.2.1 Frequency stabilized Laser 28

4.2.2 Optical bench 29

4.2.3 Phasemeter and weak-light phase locking 30

4.2.4 Telescope 31

5 Summary 31

1. Introduction

Most effectively generated in highly dynamical processes involving massive and ultra-compact astrophysical objects, gravitational waves (GWs) are unlocking a path to observe the hidden sectors of the universe with rich dynamical information. The publication of the first credible GW detection by the LIGO Scientific and Virgo Collaborations signifies the beginning of the GW astronomy Era [1]. Efforts are now being made to build more powerful detectors and to open up more GW spectrum for detection. In the high frequency end ($10 \sim 10^4$ Hz), one may expect to see Cosmic

Explorer [2] and Einstein Telescope [3, 4] detecting the merger of stellar mass compact binaries to high redshifts ($z > 2$) and at rates of one per every few minutes starting from the 2030s. In the nanohertz frequency range (around 10^{-9} Hz), indications of a possible positive detection have been reported [5, 6, 7, 8, 9]. At the lower end of the GW spectrum, efforts are being made to look for possible signatures of primordial GWs through CMB observations (see, e.g., [10, 11]). Probably the most awaited is that, in the millihertz frequency range ($10^{-4} \sim 1$ Hz), one may expect to see multiple space-based GW detectors, such as LISA [12], TianQin [13, 14] and Taiji [15], starting to operate around 2035 [16]. The Japanese DECIGO mission aims to detect GWs in the deci-Hertz frequency range [17].

Expected to be launched around 2035, the space-based GW detector TianQin aims to detect GWs in the frequency range $10^{-4} \sim 1$ Hz [13]. TianQin will be an equilateral triangle constellation consists of three drag-free satellites, orbiting the Earth with orbital radii of about 10^5 km. The detector plane of TianQin is nearly perpendicular to the ecliptic plane and the Sun will pass through the fixed orbital plane of TianQin every half year. So TianQin adopts a consecutive “three-month on + three-month off” detection scheme to protect the sensitive instruments from the direct illumination by the Sun. TianQin aims to detect a variety of astrophysical and cosmological GW sources, populating different epochs of the universe, and is expected to boost astrophysics, fundamental physics and cosmology into completely new fronts with observation data that is never seen before.



Figure 1. The “0123” technology roadmap of the TianQin Project. See main text for more explanation.

The “0123” technology roadmap (Fig. 1) has been used to guide the development of the TianQin project:

- Step “0”: To acquire the capability of lunar laser ranging, with which one can obtain high-precision orbit information for the TianQin spacecraft (S/C);
- Step “1”: To use a single satellite to test and demonstrate the inertial reference technology;

- Step “2”: To use a pair of satellites to test and demonstrate the inter-satellite laser interferometry technology;
- Step “3”: To launch a constellation of three satellites to form the space-based GW detector, TianQin, and to carry out GW detection in space.

Both step “0” and step “1” have been successfully carried out, which have prepared TianQin to precisely range to the TianQin satellites with lasers and have demonstrated the principle capability of drag-free control (DFC) for TianQin. Step “2” has been officially approved in 2021 and a pair of TianQin-2 satellites are expected to be launched around 2026 to demonstrate the inter-satellite laser interferometry technology for TianQin. Various preparation work for the step “3”, including science study, mission study and technology development, has also been carried out.

In this paper we present an update on the various aspects of the TianQin project.

2. Science Objectives of TianQin

Coordinator: Jianwei Mei

By detecting GWs in the milli-hertz ($0.1 \text{ mHz} \sim 1 \text{ Hz}$) range, TianQin is sensitive to a variety of GW sources, including:

- The revolution of Galactic compact binary (GCB);
- The inspiral of stellar mass black hole binary (SBHB);
- The Extreme Mass Ratio Inspiral (EMRI) and Intermediate Mass Ratio Inspiral (IMRI);
- The inspiral-merger-ringdown of massive black hole binary (MBHB);
- The stochastic GW background (SGWB), including those from unresolved astrophysical sources and from possible energetic processes in the early universe.

There are notable features about the types of GW signals expected for TianQin. Firstly, TianQin can detect GW sources from different epochs of the universe, for example: GCB systems in the Galaxy [18], SBHB systems to redshifts of the order $z \sim \mathcal{O}(0.1)$ [19], EMRI systems to redshifts of the order $z \sim \mathcal{O}(3)$ when the star formation rate was at its peak [20], MBHB systems to redshifts of the order $z \sim \mathcal{O}(10)$ when the first stars and galaxies just appeared [21], and possibly also first order electroweak phase transitions when the universe was only about $\mathcal{O}(10^{-10} \text{ s})$ old [22]. Secondly, TianQin can detect some GW signals with extremely high signal-to-noise ratios (SNRs). For example, SNRs for some MBHBs signals can reach the order of $\mathcal{O}(10^3)$ [21]. Thirdly, TianQin can measure the source parameters of some GW signals to extremely high precision. For example, some of the parameters of SBHBs, EMRIs and MBHBs can be measure to better in $\mathcal{O}(10^{-6})$ [19, 20, 21].

These capabilities promise a huge scientific discovery space for TianQin alone [14, 23, 24] and in joint detection with other space-based detectors such as LISA [25]. Potential scientific discoveries include: discovering massive and intermediate-mass black hole (IMBH) binary systems and compact binary systems in globular clusters; revealing the structure and material distribution of the Milky Way, the central environment of galaxies surrounding massive black holes, and the formation and evolution mechanisms of compact binary systems; high precision test of general relativity in the strong field regime; accurate characterization of the evolution history of the universe, and precise measurement of dark matter and dark energy related

parameters in a wide span of the cosmic history; and revealing the dynamics of symmetry breaking and first-order phase transition in the early universe.

2.1. Astrophysics with TianQin

Coordinator: Yi-Ming Hu

TianQin will have the ability to detect sources across a wide mass spectrum, over a wide range of cosmic history. The successful detection of the mergers of compact objects like white dwarfs, neutron stars, and massive black holes, can reveal rich information on the birth and growth of stars, galaxies and black holes. Coupled with unparalleled observation precision in parameters like mass and spin, TianQin can shed light on long-standing puzzles like the formation channel of stellar-origin black holes, seeding mechanism of massive black holes, and the stellar environments around massive black holes.

In this subsection, we aim to provide a brief overview on the detection ability of TianQin on the major types of GW sources. We discuss how the future detections, either by TianQin alone, or in coordination with other equipments, can re-shape our understanding on stellar physics, the birth and growth of massive black holes, and the immediate environment around massive black holes. A more thorough discussion can be found in [23].

2.1.1. Detection ability of TianQin

Hundreds of millions of GCB are expected to exist in our Galaxy. Even if only a tiny fraction of them are observed by TianQin, the total detection number can still reach the level of tens of thousands. Their observation and identification with the electromagnetic telescopes are challenging and only about a dozen of the known GCBs are detectable by TianQin. These are known as the verification binaries (VBs) [26]. Some VBs can have very high SNR. For example, the nominal reference source for TianQin, RX J0806.3+1527 (also known as HM Cancri, here after J0806), can accumulate SNR of 5 within two days, and exceed 100 after the five year mission lifetime. TianQin can also measure the physical parameters precisely. For examples, most of the GCBs can be localized to $\mathcal{O}(1 \text{ deg}^2)$, the frequency parameters can be constrained to the level of $\mathcal{O}(10^{-7})$, and the amplitude to the 20% level [18].

The other promising source for TianQin is the early inspiral of SBHB. Ground-based GW detectors have made hundreds of detections of SBHB mergers over the course of nearly a decade of operation and upgrade. Assuming the observed population of SBHBs, combined with TianQin's sensitivity curve, it can be deduced that a handful of SBHBs can be detected by TianQin, and the detection number can be increased either by lowering the detection threshold or by collaborating with other facilities. Many source parameters can be constrained very precisely. For examples, the merger time can be measured to $\mathcal{O}(1 \text{ s})$, the location of the source can be determined to $\mathcal{O}(0.1 \text{ deg}^2)$, and the masses can be constrained to the $\mathcal{O}(10^{-6})$ level [19, 27].

TianQin is expected to detect EMRI signals but the detection rate is subject to large theoretical uncertainties. Except for a few most pessimistic models, most theoretical models predict that TianQin can detect at least a couple of EMRI signals, with the most optimistic ones predicting hundreds of detections per year. For the detected events, all intrinsic parameters can be precisely constrained to the level of $\mathcal{O}(10^{-6})$, while the extrinsic parameters can be constrained to the 10% level [20].

TianQin also has the potential to detect the extreme mass-ratio bursts when the EMRIs are just forming [28].

There is also large theoretical uncertainty on the number of MBHB merger events that TianQin can detect. But if there is a detectable source, TianQin can detect it to the edge of the observable Universe. Even for MBHBs merging at very high redshift (such as $z \sim 15$), TianQin can still make clear detections and precise measurements of their distance and mass parameters. Apart from help revealing the origin and growth history of massive black holes, such capability can also be invaluable for exploring other aspects of the Universe, such as the global structure of the cosmic space [29]. For nearby MBHB merger events, TianQin can pinpoint the location and issue early warnings at time scales such as a day before merger [21].

SGWB contains the information of unresolvable GW events. The most obvious component is the foreground from the GCBs. With a five-year mission of TianQin, the SNR of the SGWB foreground can exceed 100 [22].

2.1.2. Stellar physics

Through detailed analysis of stellar mass compact objects, TianQin can help deepening our understanding of binary evolutions.

In the lower end of the mass spectrum, TianQin's observation of GCBs can assess the mass of compact systems, unveil the nature of the mass gap (about $2.5 \sim 5 M_{\odot}$) between the lightest black hole and the heaviest neutron stars. The large number of detections of GCBs provide a priceless catalog that can help assess the Galactic structure, tidal physics, SNe Ia progenitors, etc. In combination with electromagnetic detectors, TianQin can also increase our understanding of ultra-compact X-ray binaries (UCXBs) and AM CVns [30, 31, 32, 33].

Standard stellar evolution models predict no black holes in the mass gap at about $65 M_{\odot} \sim 120 M_{\odot}$ due to pair-instability supernova. However, GW190521 challenged this. TianQin and LISA can detect such systems in the early inspiral phase when the orbital eccentricities still carry the imprint of formation channels. By measuring these eccentricities, we can distinguish between different formation scenarios, such as those from isolated binaries with very low metallicity and hierarchical mergers between black holes/stars. Notice that the good sensitivity of TianQin in high frequency leads to an advantage in detecting SBHBs beyond the pair-instability mass gap [27, 34, 35].

In dense star environments like Pop III clusters, black holes can form hierarchical triple systems. The orbital evolution of inner binary within merging triples is different from that of isolated binaries due to the perturbation from the third object. TianQin can distinguish their formation channels by measuring the orbital eccentricities of the merging SBHBs [36]. Considering a binary moving around an massive black hole, gravitational perturbation from the massive black hole causes the inner binary to precess and may induce eccentricity oscillations. General relativity (GR) effects involving the massive black hole can generate extra precessions and change the dynamics. TianQin can observe these effects and depict the three-body dynamics [37, 38, 39].

The mergers of stellar-mass black holes could also happen in active galactic nuclei (AGN) disks. Compact objects in AGN disks can form binaries through dynamical interactions and in-situ star formation. TianQin can reveal the evolutionary processes of binaries, constrain accretion rates and binary masses, and determine the contribution of AGN channel. It can also detect the Doppler acceleration and shift of

mergers near massive black holes, unveil the locations of gaps and migration traps, and help identify potential associations of electromagnetic emissions with GWs [40, 41, 42].

2.1.3. Birth and growth of massive black holes

TianQin can help distinguish between different massive black hole seeding mechanisms. The two main models are the light-seed model, where massive black holes originate from the Pop III star remnants, and the heavy-seed model, involving the direct collapse of gas clouds. By detecting GWs from merging binary black holes across a wide range of masses, TianQin can test the predictions of different seeding models. For example, the initial mass function of seed black holes can be investigated. If Pop III stars are the main seeds, then their remnants would have relatively lower masses compared to those from direct collapse. TianQin’s ability to detect lower-mass sources in the millihertz frequency range makes it well-suited for this task [43, 44].

In colliding galaxies, IMBHs can form binaries when the clusters containing them merge. TianQin’s sensitivity to higher frequencies allows it to observe these events. By studying the dynamical evolution of IMBH binaries, such as their eccentricities and inclinations, we can learn about the dense stellar environments in which they form [25].

When massive black holes merge, there may be accompanying electromagnetic signals. TianQin’s real-time data transmission capability is crucial for enabling multi-messenger observation. By quickly identifying and localizing the source, it enables follow-up observations with electromagnetic telescopes. The pre-merger stage may show quasi-periodic variations in disk luminosity, while the post-merger stage can have changes in disk and jet luminosity due to the recoil of the new black hole. In AGN environments, IMBH binaries can produce associated flares when they merge. TianQin’s ability to work with other observatories in a multi-messenger approach can enhance our understanding of these processes [45].

2.1.4. Environment surrounding massive black holes

TianQin’s observation of EMRI and IMRI signals can reveal secrets about the sources.

Firstly, it provides insights into the existence and properties of IMBHs. By detecting light IMRIs, which consist of an IMBH and a stellar-mass black hole, TianQin can confirm the presence of IMBHs with masses in the range of $10^2 - 10^5 M_{\odot}$. The formation of IMBHs can occur through various pathways such as runaway mergers of massive stars in dense star clusters or repeated mergers of black holes in binary systems in a dense dynamical environment. Through the detection of IMRIs, one can better understand the growth processes of these black holes and their interactions within the host systems [46, 47, 25].

Secondly, TianQin can help understand the environmental effects on compact binary systems. In dense stellar systems like nuclear star clusters or globular clusters where IMRIs are expected to form, there are effects like peculiar velocity and Brownian motion. TianQin can detect the changes in the GW modes due to the peculiar velocity of the host system, which helps in determining the velocity of the source. For example, for IMRIs with different total masses, the measurability of the velocity lies in the detection of changes in non-quadrupolar modes. Also, one can detect the acceleration of IMRIs caused by Brownian motion by observing the phase shift in the GWs. This provides information about the dynamics of the star clusters and the

interaction of IMRIs with the surrounding stars [48, 49]. In addition, when IMRIs are in the accretion disks of AGNs, TianQin can detect the gas-induced dephasing effect. By calculating the orbital evolution and phase shift of IMRIs in the gas environment, we can study the interaction between the binary system and the gas. This is important for understanding the evolution of IMRIs in the AGN disks and the impact of the gas environment on the GW emission [50, 51, 52].

Finally, in multi-messenger astronomy, TianQin's detection of GW sources accompanied by electromagnetic radiation helps in identifying the host systems and the understanding of the astrophysical processes [23, 25]. For example, in the case of EMRIs and IMRIs in AGNs with a gas environment or with a star as the minor component, there can be electromagnetic radiation during or after the merger. TianQin can detect the GWs and, combined with time-domain surveys, help in identifying the host AGN. For tidal disruption events, TianQin can detect the GWs produced when a star is tidally disrupted by a massive black hole, and together with the observed electromagnetic emissions, this can help understand the disruption process and constrain the mass function of the massive black holes [53, 54].

2.2. Fundamental Physics with TianQin

Coordinator: Jian-dong Zhang

As a theory of gravity, GR has passed numerous experimental tests. However, most of the tests are performed in the weak field regime [55]. With the breakthrough in GW detection, the GW signals of binaries are used in the study of fundamental physics [56, 57, 58, 59]. The most remarkable fact about GW is that it can test the fundamental physics in the strong field regime. As a space-based GW detector, TianQin could detect some GW signals with very high SNR and precision, thus can push the test of GR to complete new fronts.

In this subsection, we summarize how TianQin can help verify the key predictions of GR in the strong field regime and search for possible signatures of beyond GR effects. We also discuss the environmental effects that may interfere with such effort. A more thorough discussion of the results can be found in [24].

2.2.1. Testing the key predictions of GR

The experimental test of GR has been going on for over a century [55]. The detection of GW has been another remarkable success for GR [56]. But only with space-based GW detection that some of the key predictions of GR can be robustly tested for the first time.

Higher modes and nonlinear modes Nonlinearity is a characteristic feature of Einstein's equations, which could be studied with GWs. The GW signal from a collapsing binary typically includes three stages: inspiral, merger and ringdown. For the early inspiral and ringdown stages, one can use the perturbation methods to obtain the waveforms.

For example, the ringdown signal after the merger of a MBHB can be expanded in terms of a series of quasi normal modes (QNMs) [60, 61, 62]. So far only GWs from the linear order have been confirmed in ground-based detectors. Among the linear modes, the (220)-mode, which has $\ell = m = 2$ and $n = 0$, is the fundamental mode, and all other modes are called higher modes and overtones. Limited by the sensitivity of existing ground-based detectors, most of the detected GW events have SNRs of 30

or less [59], while the SNRs of the ringdown phase are even weaker. Thus no higher modes has been confirmed in the existing GW data.

By using the numerically fit amplitude formulae [63], the prospect of using TianQin to detect 11 different higher modes and nonlinear modes has been studied in [64]. It has been found that some of the SNRs can reach a few dozens even for the source redshift $z = 3$. After considering three different astrophysical models, the detection numbers for each of the 11 higher modes and nonlinear modes have been analysed. Apart from the (4,3,0) mode, all other modes are expected to be detected in at least in one MBHB event.

Memory effect The radiation of GWs will result in a permanent change to the background spacetime. Such change is related to the entire history of GW radiation, and the phenomenon is referred to as the GW memory effect [65]. The memory effect is one of the direct predictions of GR in the nonlinear and strong-field regime, and so the detection of the memory effect is a direct test of GR.

The prospect of using TianQin to detect the memory effect has been studied in [66, 67]. Based on a few astrophysical population models of MBHBs, it has been found that TianQin can detect approximately 0.5 to 2 MBHB merger events for which the displacement memory effect can have SNRs greater than 3. The chance for TianQin to detect the spin memory effect from a single MBHB event is found to be negligible [66]. The memory effect can help break the degeneracy between the inclination angle and luminosity distance during parameter inference. By calculating the Bayes factor, it has been found that an SNR of approximately 2.36 is sufficient for TianQin to claim the detection of the memory effect [67].

Kerr hypothesis The no-hair theorem claims that the black holes in GR can be fully characterized by mass, spin, and electric charge. However, astrophysical black holes are believed to be nearly neutral due to several charge loss and neutralization mechanisms [68, 69, 70, 71]. Thus it's believed that the black holes in our universe can be described by the stationary and rotating Kerr metric [72]. This is called the Kerr hypothesis. With GWs, high-precision tests of the Kerr hypothesis can be conducted through different ways, such as detecting the ringdown signal of a black hole [73] and measuring the multipole moment of a black hole [74].

If GR and the Kerr hypothesis is valid, the oscillation frequencies and damping times of the QNMs are entirely determined by the mass and spin of the final Kerr black hole. One can test the Kerr hypothesis by measuring multiple frequencies and damping times of the QNMs, and check if they correspond to the same mass and spin. The oscillation frequency ω_{lmn} and the damping time τ_{lmn} can be parameterized as:

$$\omega_{lmn} = \omega_{lmn}^{GR}(1 + \delta\omega_{lmn}), \quad \tau_{lmn} = \tau_{lmn}^{GR}(1 + \delta\tau_{lmn}) \quad (1)$$

where the deviation parameters $\delta\omega_{lmn} = \delta\tau_{lmn} = 0$ if GR is correct. For TianQin, the combination of $\delta\tau_{22}$, $\delta\omega_{22}$, and δw_{33} offers the most stringent constraint for vast majority of cases. With the consideration of three astrophysical models, the selected deviation parameters can always be constrained to the 1% level or better, and some can even reach the $\mathcal{O}(10^{-4})$ level [75].

For an isolated massive object, its gravitational field can be characterized by its multipole moments. The multipole moments of a Kerr black hole are fully determined by its mass M and spin a :

$$M_l + iS_l = M(ia)^l, \quad l = 0, 1, 2, \dots \quad (2)$$

To test if an astrophysical black hole is a Kerr black hole, one can measure the quadrupole moment with $l = 2$, in addition to the mass and spin. One can parameterize such test by treating the quadrupole moment as an additional parameter, $Q = -(1 + \delta\kappa)a^2M$. $\delta\kappa$ is a deviation parameter depending on the internal structure of the object, and it equals to 0 for Kerr black holes. The prospect of using TianQin to measure the Kerr quadrupole moment has been studied in [76, 77]. Using MBHBs, TianQin can constrain $\delta\kappa$ to the order $\mathcal{O}(10^{-2})$, and the events with asymmetric mass will have better capability. It has been found that TianQin can constrain $\delta\kappa$ to the order $\mathcal{O}(10^{-6})$ using EMRIs. Comparing to the mass, the spin of the central black hole has a more significant impact on the constraints, and the larger the spin, the stronger the constraints.

2.2.2. Looking for possible signatures of beyond GR effect

If GR is not fully correct, one may hope to find some beyond GR effect in GW emission, including the fundamental degrees of freedom of GWs, the generation and propagation of GWs. The possible beyond GR effects can be searched with various parameterization schemes, with various modified gravitation theorys (MGTs) being representative examples. Current studies have not found any deviations from GR, but TianQin can push the tests to new frontiers.

GW polarization In GR, GWs possess only two tensor polarization modes. But for a general metric theory of gravity, the metric tensor has 6 propagation degrees of freedom, thus there can exist 6 polarization modes [78, 79]. These additional polarization modes can be excited by the coupling between the metric and extra gravitational fields.

For the GW events detected by ground-based detectors, a Bayesian model selection analysis shows that the data supports the assumption that the signals are consisted of purely tensor modes, rather than purely vector or scalar modes [80, 57, 81]. The null-stream method has been used for the O2, O3a and O3b events, and all the data is consistent with the pure tensor mode hypothesis [82, 83].

TianQin is expected to detect about 10^4 pairs of GCBs [18] and the prospect of using TianQin and GCB signals to search for extra polarization modes has been studied in [84]. Due to the vanishing of the antenna pattern function, TianQin has no detection power for the vector or scalar modes for sources located in the direction of J0806 and its antipodal point. For sources located in other directions, the best precision on α_v can reach the 2% level and that for α_s can reach the 5% level, where α_v and α_s are the relative magnitudes of the vector and scalar modes compared to the two GR modes, respectively. VBs with known position can produce better constraints, and ZTF J1539 is currently the best among all the VBs.

The MBHB signals can also be used to constrain the extra polarization modes, and the correction on the phase evolution must be considered in the waveform. In a preliminary study with the Bayes method, the constraint with TianQin on the amplitudes of extra polarization modes has been found to be about a few percent [85]. The possibility of using SGWB to constrain the extra polarization modes has been studied in [86, 87].

GW propagation In GR, GWs travel at the speed of light. But GWs in MGTs may propagate differently than the speed of light. In general, we can consider a non-trivial

dispersion relation for GWs as

$$E^2 = p^2 + \mathbb{A}_\alpha p^\alpha, \quad (3)$$

where E and p are the energy and momentum of the graviton, respectively. α is a power and \mathbb{A}_α is the corresponding magnitude of modification. In GR, $\mathbb{A}_\alpha = 0$. For $\alpha = 0$, one usually writes $\mathbb{A}_0 = m_g^2$, where m_g corresponds to the graviton mass. The analysis of the GWTC-1 [88], GWTC-2 [89] and GWTC-3 [90] data has set the bound to $m_g \leq 1.27 \times 10^{-23}$ eV. The current bound on \mathbb{A}_α for $\alpha \in [0, 4]$ can be found in [57, 58, 59].

A preliminary study shows that TianQin can probe the graviton mass to $m_g < \mathcal{O}(10^{-27}$ eV), thus improving over the current bound on graviton mass by four orders. TianQin can also improve over the current bounds on \mathbb{A}_0 , $\mathbb{A}_{0.5}$ and \mathbb{A}_1 by about eight, five and three orders, respectively [24].

GW generation The parameterized post-Einsteinian (ppE) framework has been developed to enable a theory agnostic probe of possible deviations from GR [91, 92, 93, 94]. The basic idea of ppE is to focus on the leading post-Newtonian (PN)-order corrections to the PN waveform,

$$h_{\text{ppE}}(f) = h_{\text{GR}}(f)(1 + \alpha u^a)e^{i\beta u^b}, \quad (4)$$

where α and β are the ppE parameters, with $\alpha = \beta = 0$ in GR, and a and b are the PN-order parameters, with $b = k - 5$ and $a = b + 5$ corresponding to the $(k/2)$ PN order. The ppE parameters for a given MGT can be found by computing the corrections to the orbital evolution of the binary system [95]. Using this approach, ppE parameters have been determined for a spectrum of theoretical models, See [95, 96] for a summary.

The prospect of using TianQin to test MGTs with the ppE formalism has been studied in [97]. The result shows that $\Delta\beta$ is more tightly constrained by the low-mass sources at the lower PN orders, while $\Delta\beta$ at the higher PN orders are best constrained with the sources at around $\mathcal{O}(10^5 M_\odot)$. The prospect of testing specific MGTs has also been studied. With the detection of SBHBs with total masses below $M < \mathcal{O}(10^2 M_\odot)$, TianQin is expected to constrain EdGB to the order $\sqrt{|\bar{\alpha}_{\text{EdGB}}|} < \mathcal{O}(0.1 \text{ km})$, which is about one order better than the current best result. Similarly, TianQin is expected to constrain dCS to the order $\sqrt{\bar{\alpha}_{\text{dCS}}} < \mathcal{O}(1 \text{ km})$. In the case of non-commutative gravity, TianQin is expected to improve over the current best bound by an order of magnitude and constrain the theory to the sub-Planckian scale. For \dot{G} , TianQin can push the constraint to the level of $|\dot{G}/G_0| < \mathcal{O}(10^{-5} \text{ year}^{-1})$. For more details, we refer to [97].

2.2.3. Environmental effects

In searching for possible signatures of beyond GR effect, an important issue is to avoid mistaking false signals for evidence of new physics. Around the GW radiating binary sources, there may exist accretion disks, dark matter halos, or third gravitational bodies. The surrounding matter can change the orbit evolution due to the gravitational pull and dynamical friction, or change the mass and spin of the sources due to the accretion of surrounding matter. On the path of the GW propagation, there can exist different density of matter, causing gravitational lensing effect for GWs. Depending on the density profile of the lenses, GW can be bent, delayed, (de)magnified, phase-shifted, and diffracted. In real GW detection, the environment is not known. So the problem is how to distinguish between the environmental effect and possible signatures of beyond GR effect.

Environmental effect in GW generation The capability of TianQin in probing the environmental effect during GW generation can be directly obtained from the ppE result (see subsection 2.2.2). For example, the dynamical friction due to a dark matter spike with density profile $\rho_{\text{DM}} = \rho_0(r_0/r)^{3/2}$ affects the inspiral signal at the -4 PN order, which is the same as the effect of \dot{G} . To distinguish these two effects, one can define the following function,

$$F = \sum_{i=1}^n \frac{(\dot{G}_i - \bar{\dot{G}})^2}{\sigma_i^2}, \quad (5)$$

where n is the number of detected events and the index i means the i -th event, \dot{G}_i and σ_i are the mean value and variance of \dot{G} for the i -th event. $\bar{\dot{G}}$ is the mean value of \dot{G}_i for all the events. By using a specific astrophysical population model for binary black holes, one can find that F will be small if the waveform correction is due to the varying- G , while F is very large if the correction is due to dark matter halo [98]. This result shows that it is possible to distinguish these two effects if multiple events are detected.

Environmental effect in GW propagation When electromagnetic waves pass by a massive object, there will be gravitational lensing effect. Similar to electromagnetic waves, GWs can also be lensed [99]. If the lensing effect is not properly included in the analysis of GW data, there can be systematic errors in the estimation of source parameters [100]. What's more, lensed GW signals can be used to study the propagation property of GWs, infer the physical properties of the lensing object, study the nature of dark matter and the expansion of the universe.

So far the LIGO-Virgo-KAGRA collaboration has published 90 GW events [101]. Despite much effort, however, no lensed GW signal has been confirmed in these events [102]. Recent study suggest that nearly one percent of the detected events for TianQin may experience strong gravitational lensing [103]. It is also possible for wave-optics effects of lensing to be detected [104, 105], if the GW wavelength is comparable or longer than the gravitational radius of the lens.

The prospect of using TianQin to probe the gravitational lensing effect for GWs has been studied in [106]. The result shows that the gravitational lensing increases both the SNR and the precision of parameter estimation. The parameter of the lens can also be measured with an accuracy of $\mathcal{O}(10^{-5})$ or better.

2.2.4. New fundamental matter and interactions

Coordinator: Fa Peng Huang

In this part we discuss the prospect of using TianQin to probe possible new physics in the non-gravitational sector. To explain the origin of matter-antimatter asymmetry in the observable universe and the microscopic nature of dark matter, it is often necessary to introduce new fundamental particles and interactions beyond the Standard Model of particle physics. Over the past few decades, experimentalists have not observed these new particles or interactions in dark matter direct detection experiments, collider experiments, or other related studies. This may suggest the need for experimentalists to explore new experimental approaches. As a space-based GW detector, TianQin could open a unique and novel window to probe such new fundamental matter and interactions.

Probing the nature of dark matter Dark matter may directly generate GW signals during its production in the early universe or leave significant imprints on GW signals throughout its astronomical evolution. Based on the current state of experimental and theoretical research on dark matter detection, attention has shifted toward studying ultralight or superheavy dark matter. TianQin has the potential to detect these two types of dark matter candidates through GW signals.

Boson clouds formed by dark matter particles like axions through superradiance around black holes can affect the orbital evolution of binary black holes and neutron star-black hole systems, altering the GWs of such events [107, 108, 109, 110, 111, 112]. These effects can be used to reveal dark matter properties near black holes through GW detection [113, 114, 111, 112]. Scalar and vector boson clouds can also emit GWs directly via pair annihilation of bound-state particles and energy-level transitions [115, 110, 116]. The GW signal from boson clouds is quasi-monochromatic, with frequency depending on the boson particle mass. These GWs can be detected individually by ground-based and space-based observatories [117, 118, 119, 120, 121, 122], and they can also contribute to the stochastic background [117, 118, 123, 124]. For example, the axion cloud's effect on binary GWs can be detected by TianQin.

In the early universe, the production of dark matter is often accompanied by the generation of GWs. Therefore, GW experiments like TianQin can provide novel methods for probing the properties and production mechanisms of dark matter. Different dark matter models predict different phase transition parameters, such as the phase transition strength [125], phase transition duration, and the bubble wall velocity [126, 127, 128, 129]. Phase transitions also offer new mechanisms for dark matter production, including filtered dark matter [130, 131, 132], soliton dark matter [133, 134, 135, 136, 137], and so on.

Interpreting GW data to understand dark matter properties is complex, necessitating detailed modeling of both GW sources and dark matter interactions. Additionally, distinguishing potential dark matter signals from other astrophysical sources requires highly sensitive and precise measurements.

Probing the origin of matter-antimatter asymmetry of the universe and the new Higgs potential After the discovery of the Higgs boson, exploring the shape of the Higgs potential has become a critical issue in particle cosmology. It also provides essential conditions for explaining the origin of matter-antimatter asymmetry in the universe. A generic new physics model with new particles and new interactions would prediction new Higgs potential in the form of the dimension-6 operators [138, 139, 140, 141, 142]. This new Higgs potential can induce a strong first-order phase transition in the early universe and provide the necessary condition for the electroweak baryogenesis mechanism that naturally explains the origin of matter-antimatter asymmetry. TianQin is expected to be capable of probing new physical models or new Higgs potential functions that can produce first-order electroweak phase transitions in the universe. Specifically, it can probe the parameter space of new physical models with a phase transition strength greater than 0.1, namely, $\alpha > 0.1$.

Various theoretical models have been proposed to explain matter-antimatter asymmetry through mechanisms involving GWs. Each model predicts specific GW signals that can be tested by future observations. Mechanisms for achieving baryogenesis include electroweak baryogenesis, leptogenesis, and first-order phase transitions in the early universe. These often predict distinct GW signatures detectable by various observatories. The GW signals from phase transitions provide a

direct probe of early universe conditions leading to baryogenesis, with different models predicting varying GW spectra based on phase transition specifics.

2.3. Cosmology with TianQin

Coordinator: Liang-Gui Zhu

After nearly a century of development, current cosmological research has entered the era of precision cosmology. The standard model of cosmology — the cosmological constant cold dark matter (Λ CDM) model, describes well most of the cosmological observations from primordial nucleosynthesis to the present. However, the Λ CDM model is not perfect. As the precision of measurements of various cosmological parameters improves, the Λ CDM model faces several challenges, the two most notable of which are: (i) the inconsistencies in measurements of the Hubble-Lemaître constant (H_0) from different probes (commonly referred to as the Hubble tension) [143, 144, 145, 146, 147, 148, 149, 150, 151] and (ii) the significant deviation of the dark energy equation of state from the cosmological constant [152, 153, 154]. These challenges may suggest anticipated new physics beyond Λ CDM, but one thing that is more important before exploring candidate new physics is to confirm the existence or clarify the source of these challenges.

GW detections allow us to directly estimate the luminosity distances of compact binary GW sources to us without the need for calibrations of the cosmic distance ladder, and the combination of luminosity distance information from GW detections and redshift information obtained by other means can be used to independently probe the expansion history of the Universe, so GWs are known as *standard sirens* [155, 156, 157]. The LIGO & Virgo network first realised the idea of probing the cosmic expansion history using standard sirens through their detected GW events [158, 159, 160]. The network of current ground-based GW detectors has measured H_0 with a precision of about 10%, but has yet to provide an effective constraint on the equation of state of dark energy [101], thus more GW detection plans are needed to shed light on the challenges faced by Λ CDM through GW standard siren probes. Space-based GW detectors in milli-Hertz band are expected to be launched in the 2030s [12, 13, 14, 15], the types of candidate sources that can be detected will be more diverse [161, 23], so that the constraints on the cosmic expansion history from different types of candidate GW sources can be complementary and calibrated with each other [162], thus space-based GW detections will be able to provide irreplaceable roles in clarifying the Hubble tension and in probing the nature of dark energy.

TianQin can detect several types of candidate standard sirens, namely, SBHB inspirals [163, 164, 165], EMRIs [166, 167, 168] and MBHB mergers [169, 170, 171]. The sensitive frequency band of TianQin is a bit higher than that of LISA, and there is a long baseline between the detectors of TianQin and LISA, so TianQin and LISA can complement each other well [172, 173, 19, 174, 20, 25].

In this subsection, we will briefly introduce the potential of TianQin for probing the expansion history of the Universe, including measuring the parameters of the Λ CDM model and the equation of state of dark energy. A more thorough discussion of the results can be found in [24].

2.3.1. Constraining the Λ CDM model

The three types of candidate standard sirens for TianQin — SBHBs, EMRIs, and MBHBs, are distributed at low ($z < 0.3$), medium ($z \lesssim 2$), and high ($z \lesssim 10$)

redshifts, respectively, forming a *probe ladder* to better constrain the Λ CDM model. For SBHB inspirals and EMRIs, current studies generally assume that they have no observable electromagnetic (EM) counterparts, requiring the statistical determination of their redshift information by cross-matching them with surveyed galaxy catalogs [163, 164, 166, 167]. For MBHBs, the presence or absence of observable EM counterparts, as well as their characteristics, depend heavily on the astrophysical environments surrounding the GW source [169, 170, 175].

Since the low redshift GW sources detectable by TianQin include all three types of SBHB, EMRI and MBHB sources, all three types of sources are effective in constraining H_0 [165, 168, 171]. The precision with which TianQin constrains H_0 using the SBHB detections is expected to be around 20%, potentially improving to about 8% with the TianQin I+II configuration [165]. These precisions are comparable to those achieved by the current network of ground-based GW detectors [101], with the level of precision primarily limited by the low SNR of SBHB inspiral signals. If TianQin and the next generation ground-based GW detectors (such as Einstein Telescope and Cosmic Explorer [176, 177]) can form a multi-band network, a constraint on H_0 of 1% precision level can be achieved using only about one hundred SBHBs [165]. The expected precision with which TianQin can constrain H_0 using EMRI detections is about 1% – 8% [168]. Such large uncertainties arise primarily from our limited understanding of the EMRI event rates, which are affected by factors such as the population of massive black holes at the centers of galaxies, stellar cusps surrounding the massive black holes, the mechanisms by which massive black holes capture stellar-mass objects [178, 179], and activities of the massive black holes [180, 181, 182]. The expected precision for TianQin to use MBHB signals to constrain H_0 is about 1.5% – 6% in the optimistic scenario and about 2% – 7% in the conservative scenario [171, 183]. The uncertainties in the predictions are again caused by the uncertainty in the MBHB event rates [184, 21].

The prospect of using TianQin to constrain other Λ CDM model parameters, such as the fractional total matter and dark energy density parameters Ω_M and Ω_Λ , is mainly rooted in the EMRI and MBHB detections [168, 171]. Regardless of the type of GW sources used, both the constraints of TianQin on Ω_M and Ω_Λ are expected at the dozens of percent level, reaching the 10% level only in very optimistic scenarios [168, 171]. Although the precision on Ω_M and Ω_Λ is not very high here, doing a simultaneous estimation of these parameters can avoid the biases in H_0 estimations.

Two of the most representative H_0 measurements signifying the Hubble tension are: 67.4 ± 0.5 km/s/Mpc inferred by the Planck Collaboration with cosmic microwave background (CMB) observations plus the Λ CDM model [143], and 73.04 ± 1.04 km/s/Mpc obtained by the SHOES Team with Type Ia supernova (SN Ia) observations plus cosmic distance ladder [144], corresponding to relative precisions of about 1.4% and about 0.7%, respectively. To help break the draw, TianQin will need to provide an independent H_0 measurement with a precision better than about 2%. This is possible with the three types of standard sirens, SBHB, EMRI and MBHB, but with some strings attached: using SBHB detections is dependent on the implementation of a multi-band network [165], and using EMRI or MBHB detections is dependent on their event rates [168, 171]. To help improve the constraints on H_0 with a given set of GW signals, it is necessary to optimise the data processing process. Some candidate optimisation methods include: (i) for SBHBs, weighting candidate host galaxies with photometric information in all bands contained in the galaxy catalogs [165]; (ii) for EMRIs, inferring the correlation between EMRIs and AGNs by statistical methods

[168]; (iii) for MBHBs, weighting candidate host galaxies with the correlation between the massive black hole masses and bulge luminosity of galaxies [171]; (iv) for lensed MBHBs, extracting the redshift information of GW sources directly using the strong gravitational lensing effect [185]; and (v) for all three types of GW sources, decreasing the spatial localization error volume by the combined data analysis of TianQin and other detectors [173, 19, 174, 20, 25, 21]. These methods can improve the precision of H_0 ranging by a few percent to several times [165, 168, 171, 185].

2.3.2. Probing the equation of state of dark energy

Dark energy drives the transition of the cosmic expansion from deceleration to acceleration. A typical phenomenological dark energy model is the Chevallier-Polarski-Linder (CPL) model [186, 187], which has two parameters, w_0 and w_a , describing the redshift-independent constant part and the redshift-dependent variable part of the dark energy equation of state, respectively. The cosmological constant is the simplest dark energy model and the current standard in the Λ CDM model, corresponding to a constant equation of state of $w \equiv -1$ (i.e., $w_0 = -1$ and $w_a = 0$ in the CPL model) [188, 189, 190]. The latest observations of the dark energy equation of state published by the Dark Energy Spectroscopic Instrument (DESI) shows a significant deviation from the cosmological constant, with the most significant deviation coming from a combined constraint of CMB, BAO and SN Ia observations, yielding $w_0 = -0.73 \pm 0.07$ and $w_a = -1.1 \pm 0.3$ [154]. The corresponding relative precision of the parameter w_0 is about 10%.

Constraining the equation of state of dark energy requires combining observations at different redshifts. Thus, TianQin's ability to constrain the dark energy equation of state primarily relies on EMRI and MBHB events whose distributions span from low to high redshifts [168, 171]. TianQin's expected precision for constraining the parameter w_0 using EMRI detections is $|\Delta w_0/w_0| \sim 5\% - 40\%$, but obtaining an effective constraint on w_a is challenging [168]. Using MBHB detections, TianQin can achieve effective constraints on both w_0 and w_a in the optimistic scenario with EM counterpart observations, with expected precisions of $|\Delta w_0/w_0| \sim 7\% - 14\%$ and $\Delta w_a \sim 0.4 - 0.6$ for w_0 and w_a [171]. However, in the conservative scenario without EM counterpart observations, TianQin can only constrain w_0 , with an expected precision of $|\Delta w_0/w_0| \sim 10\% - 40\%$. Similar to the constraints on H_0 , the uncertainties in the expected constraints on the parameters w_0 and w_a by TianQin are also due to the uncertainties in the population models of EMRIs and MBHBs [168, 171]. As with the constraints on H_0 , optimising data processing method can also improve the precisions on the equation of state of dark energy [168, 171].

3. Concept and design of TianQin

Coordinator: Xuefeng Zhang

The concept of TianQin is to deploy three satellites in circular high Earth orbits with a radius of about 10^5 km, forming a nearly equilateral-triangle constellation. The satellites exchange laser interferometric links to detect GWs in the mHz frequency band. The constellation plane is nearly fixed and set almost vertical to the ecliptic, facing the verification source RX J0806.3+1527. Due to varying solar angles relative to the constellation plane, the operation scheme consists of having two separate 3-month observation windows within a year when the Sun is roughly facing the constellation plane [13] (see Fig. 2).

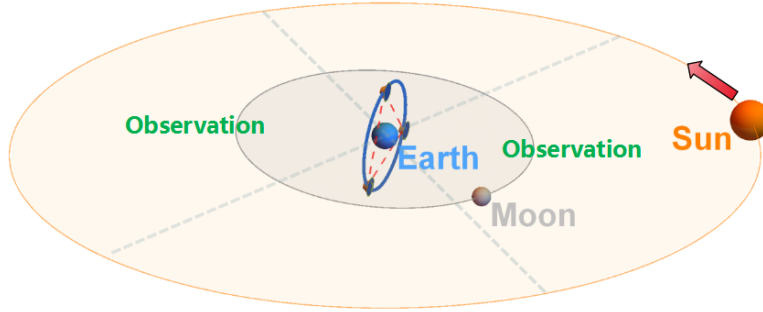


Figure 2. The TianQin constellation viewed in the Earth-centered celestial frame (not to scale). The dashed lines mark the two 3-month observation windows when the Sun is roughly facing the orbital plane.

TianQin features a geocentric concept. This choice of orbits has far-reaching influence on the mission and system design. The design needs to take into account several main aspects and their interplay, these including science objectives, orbits and constellation, space environment, science payload, satellite platform, etc. At the time of the first proposal [13], a well-rounded solutions applicable to TianQin was not present in the literature.

3.1. Special challenges

Being close to the Earth has major benefits, e.g., launch and deployment, data communication, telecommand, navigation, etc. These can help mitigate engineering risks and technical difficulties. However, there have also been serious concerns and challenges to the feasibility of geocentric missions in general (see, e.g. [191]). We name the main five of them:

- Constellation stability;
- Eclipses due to the Moon and Earth;
- The Earth and Moon’s gravity disturbance to science measurements;
- Varying thermal environment; and
- Solar-wind plasma disturbance to science measurements.

In the following, we will briefly review the answers or solutions to these issues, based on the intensive and focused studies carried out so far [192, 193, 194, 195, 196, 197, 198, 199, 200, 201, 202, 203, 204, 205, 206, 207], which have also been recently summarized in [208].

3.2. Orbit and constellation

Gravitational perturbations from celestial bodies such as the Moon and Sun, along with orbit control errors, cause the S/C constellation to deviate from its nominal equilateral triangle configuration. There are three key performance indices of stability: variations in armlengths, relative velocities, and breathing angles. The stability of the constellation is crucial and affects several aspects of science payload design such as laser pointing control, phase measurement, laser frequency noise removal, payload architecture, etc. To alleviate pressure on instrumentation, it would be desirable to

find orbits with deviation from the equilateral triangle as small as possible. Through optimization techniques for pure-gravity orbits, the constellation can be stabilized to armlength variations within $\pm 0.1\%$, relative velocity changes within ± 4 m/s, and breathing angle fluctuations within $60 \pm 0.1^\circ$ over two years [192, 193]. The natural fluctuation of breathing angles caused by gravitational perturbations is estimated to be $\pm 0.06^\circ$, leaving margins for orbit determination and control. Additionally, the detector pointing is quite stable, varying by $< 3^\circ$ over five years. Moreover, the implications for time delay interferometry (TDI) have been studied, and it indicates that the first-generation TDI is applicable to TianQin due to a small residual armlength mismatch [194], which can make data processing on the ground easier.

Eclipse avoidance is important for TianQin due to potential thermal shocks and power disruption to the satellites by traversing Moon and Earth’s shadows. This was considered a major risk for geocentric concepts [191] with remedies not well studied. To address the issue, an eclipse-free orbit design was proposed to ensure that the satellites do not undergo Moon eclipses during the observation windows of $3 + 3$ months [209]. Although Earth eclipses are unavoidable, they occur outside these windows, hence less worrisome. The design proposes 1:8 synodic resonant orbits with respect to the Moon, which is to have the satellites to complete eight revolutions in one lunar month. The idea is to set the satellite motion in a repeated phase relation with the Moon’s shadow to reduce the possibility of Moon eclipses. An optimal orbital radius of 100,935 km has been identified for a launch in the early 2030s. The resulting optimized orbits can avoid all eclipses in $3+3$ months observation windows for a 5-year mission and meet the constellation stability requirements. Additionally, eclipse-free observation windows can be further extended to $4+4$ months at an acceptable expense of reduced allowed ranges of initial phases of the satellites.

The mission orbit design needs to take into account and balance among a variety of factors such as science objectives, constellation stability, space environment, science payload, launch capability, etc. Each design factor may have its own preference. Based on our current trade-offs, the mission orbit is proposed to have a semimajor axis of $a = 100935$ km, eccentricity $e < 0.002$, inclination $i = 94.7^\circ$, and ascending node $\Omega = 210.4^\circ$ in Earth-centered ecliptic coordinates [195, 209, 197, 210]. To keep the constellation stable for at least 3 months, typical initial orbit error requirements are ± 20 m in the radial position and ± 2 mm/s in the along-track velocity, which will be addressed in Sec. 3.5. The three satellites are foreseen to be delivered by one single heavy-lift launch vehicle into an elliptical transfer orbit, then reaching their final orbits by raising the perigees.

3.3. Space environment

Gravitational disturbances from Earth and Moon may significantly affect the geodesic motion of test mass (TM) in the inertial reference systems, potentially inducing “orbital noise” similar to Newtonian noise observed in ground-based detectors. To assess the “quietness” of the ambient gravitational field, we have chosen the range accelerations between TMs to perform the evaluation. The criteria for this assessment involve comparing the amplitude spectral density of the residual acceleration noise between two TMs, with the requirement of $\sqrt{2} \times 10^{-15}$ m/s²/√Hz in the frequency range of 10^{-4} Hz to 1 Hz. Achieving this precision necessitates the use of quadruple precision to propagate pure-gravity orbits. From careful modeling and simulation, the total gravitational disturbance is expected to dominate only at lower frequencies and

drop below the requirement at 1×10^{-4} Hz, hence not presenting a showstopper to the mission [196, 198, 199]. By positioning the satellites at an orbital radius greater than 1×10^5 km, these disturbances can be pushed out of the sensitive frequency band [197].

The thermal environment is crucial for the performance of inertial sensors and laser interferometers, necessitating stringent requirements of the level 10^{-5} K/ $\sqrt{\text{Hz}}$. A primary challenge for TianQin stems from the varying direction of sunlight relative to the constellation plane, which can introduce thermal variations that may impact instrument performance. To mitigate these effects, a flat-top sunshield design was proposed [201], adapted from science missions such as WMAP, Gaia, JWST, LISA, and LPF. The design ensures that no other parts of the satellite are directly exposed to sunlight, allowing steady heat pathways from the top to the bottom and sides of the satellite. Consequently, the design effectively shifts solar flux variations to a half-year period, minimizing their influence on the instruments. Within the detection band, fluctuations of the solar constant dominate for TianQin [202]. This underscores the importance of robust thermal control for maintaining the desired operational temperature range and stability, which is critical to the overall success of the mission.

The interaction of solar-wind plasma with laser propagation between the satellites was suspected to induce extra phase noise, affecting the precision of interferometric measurements. To evaluate this effect, magnetohydrodynamic simulations have been conducted using the Space Weather Modeling Framework along with observational data from the OMNI database [211]. The results indicate that the induced phase noise stays below the allocated noise budget of approximately 30% of the total noise, except during strong solar storms that can raise the level [204, 207]. Furthermore, it was found that the application of TDI combinations can effectively mitigate the noise effect. Specifically, TDI is able to achieve about 50% noise suppression in the frequency range below 10^{-2} Hz. This noise suppression is primarily due to the noise correlation among the three arms of the interferometric setup [205, 206]. Thus, the influence of solar-wind plasma is fairly understood for the operation and performance of TianQin.

3.4. Science payload

The choice of the payload architecture and pointing control strategy is crucial, particularly considering the Earth-Moon environment faced by TianQin [212]. The core payload comprises the telescope, optical bench, and inertial sensors, rigidly connected to one another, and the in-plane pointing is achieved via single-axis rotation of the optomechanical assembly, while off-plane pointing is managed through satellite attitude control [12]. The alignment of the optomechanical assembly axes and TMs with respect to received beams is facilitated by differential wavefront sensing to achieve an accuracy in the order of 10 nrad. The coupling of orbit and attitude needs careful consideration, as changes in orbit affect the pointing and attitude control. Under breathing angles of $60 \pm 0.1^\circ$ and constellation plane variations of $\sim 0.05^\circ$ per orbit, the nominal force and torque for TM suspension control are estimated to be well below the budget, where the acceleration noise requirement mandates the control acceleration below 10^{-10} m/s² and angular acceleration below 10^{-10} rad/s². Moreover, control forces can be minimized by positioning of the satellite's center of mass at the midpoint between TMs [212].

The point-ahead angle control is a critical aspect in accurate laser pointing

between satellites by addressing delays from the finite speed of light. The point-ahead angle, defined as the angle between the received and transmitted beams, is fully determined by the satellite orbits. Orbit simulation for TianQin has established an in-plane static bias of 23 μrad , with variations of ± 25 nrad in-plane and ± 10 nrad off-plane. Hence, a fixed-value compensation strategy can be adopted to absorb small and slow variations into pointing biases up to ± 35 nrad [213]. From the far-field tilt-to-length (TTL) coupling with a pointing jitter of $10 \text{ nrad}/\sqrt{\text{Hz}}$, the requirement on far-field wavefront quality has been derived accordingly. A preliminary TTL calibration procedure using null TDI channels has been put forward and assessed via numerical simulation [214]. The strategy has major benefits in simplifying interferometer design, payload operation, and TTL noise mitigation.

To help with performance assessment and noise budgeting, the team has also developed TDI and data pre-processing simulation tools (TQTDI) [200]. The simulation utilizes sub-pm/ $\sqrt{\text{Hz}}$ orbits from TQPOP [196] and multi-body attitudes from TQDYN [212, 215] to generate more realistic heterodyne beatnote signals, capturing the complex dynamics of the satellites and the constellation. Additionally, to remove Doppler shift due to Earth-Moon's gravitational disturbances, a high-performance high-pass filter is implemented, which is shown to be compatible with TDI. These techniques enhance simulation fidelity and aid in more accurate analyses.

3.5. Satellite platform

Coordinator: Xuefeng Zhang, Ming Li, Lihua Zhang

The satellite platform is engineered to fulfill strict requirements in thermal, magnetic, self-gravity, structural, and vibrational aspects, which requires a customized design that addresses both external and internal environmental challenges in space (see, e.g. [216]). The preliminary configuration features a single flat-top sunshield, thermally isolated to provide over three months of effective shading [201]. The octagonal squashed outer shape, along with central support and shear panels, helps to enhance structural rigidity [217, 203]. Additionally, the compartmentalized and symmetric layout aids in mass balancing and self-gravity mitigation.

The thermal design of the satellite aims to maintain stable operating temperatures despite significant solar angle and thermal flux variations that can reach approximately 38% over three months. Following passive thermal guidelines, the preliminary design incorporates a sunshield and top-plate equipped with optical solar reflectors, polyimide foams, gold coatings, and aerogel for enhanced insulation. The simulation results show that the key payload bay can maintain a slight variation of < 2 K over three months [203]. Due to the importance of thermal control, further discussion is deferred to a separate subsection (Sec. 3.6).

The satellite employs cold gas thrusters to execute drag-free operations and precise pointing control, particularly under varying solar radiation pressure, both seasonally and in orbital periods. To avoid plume impingement, the thruster directions are limited, and they are oriented downward and away from the sunshield and satellite body, with solar radiation pressure as a virtual thruster. Both 3-cluster and 4-cluster designs have been tested [212]. Allocation of the required total force and torque indicates positive-output solutions can be achieved for four months in the science mode, ensuring consistent drag-free and pointing accuracy throughout the mission. Furthermore, electric propulsion with higher thrusts is also foreseen to assist precise orbit control during non-observation periods.

Other features of the satellites include Global Navigation Satellite System (GNSS) receivers and real-time data downlink. The former is adopted for precise orbit determination using GNSS leak signals, which has the advantages of reducing ground-based tracking infrastructure costs and receiving real-time data [218]. Previously tested in Chang'e missions, it is estimated that the method has an accuracy of 4.8 m in radial position and 0.2 mm/s in along-track velocity over a seven-day arc [219], which can meet the requirement. GNSS can also be used jointly with satellite laser ranging [220, 221] and other methods for further improvement [222]. For data communication, a high-gain antenna is to be installed to the front panel of the satellite and can remain fixed and automatically Earth-pointing in the science mode, and provide a data rate greater than 1 Mb/s. Additionally, data can be relayed via laser links to at least one satellite visible to the ground, enabling continuous real-time downlink to support quick alerts of important merger events, thereby enhancing mission responsiveness [223].

3.6. Thermal control

Coordinator: Ran Wei, Xin Zhao

The thermal control subsystem is an important component of the entire satellite. To achieve the μK -level temperature control required by the core payload, developing the thermal control subsystem needs research on mechanism for temperature noise transmission and attenuation, high-resolution temperature measurement theory, and ultra-low noise active suppression methods, breaking through core technologies such as temperature noise suppression, high-precision temperature measurement sensing, and test verification.

Research has been carried out on the temperature noise suppression technology exploring the transmission and attenuation mechanisms of different frequency disturbances in the thermal structure. It constructs a multi-level temperature control system model using control equations based on time constants and validates it with a damping oscillation model based on the theory of heat and mass, providing a design method for multi-level energy attenuation control. Combining the configuration layout, flight attitude, and orbital characteristics of TianQin, a high-precision thermal network model is constructed using a hierarchical approach, and some preliminary result on the energy flow and temperature distribution of the satellite has been obtained. Through comparative analysis of the finite difference thermal network model and the multi-coupled thermal effect model of the high vacuum ($\leq 10^{-6}$ Pa) region around the inertial sensor TM, the frequency-domain thermal analysis results around the inertial sensor TM are obtained [224, 225, 226, 227, 228, 229, 230]. The results show that the temperature noise of the TM part can be controlled below $5 \mu\text{K}/\text{Hz}^{1/2}$.

In engineering, to achieve μK -level temperature measurement, the ultra-low-frequency noise estimation and separation technology based on multi-channel cross-spectrum circuits and the isolation power supply and bidirectional drive differential proportional ultra-high-resolution temperature measurement technology have been developed. In the frequency band of 0.1 mHz to 1 Hz, the equivalent temperature noise spectral density in the laboratory has reached $9 \mu\text{K}/\text{Hz}^{1/2}$, and the goal of $2 \mu\text{K}/\text{Hz}^{1/2}$ is being pursued [231, 232, 233, 234, 235, 236, 237, 238]. To eliminate the influence of long-period thermal flow disturbances, a low-frequency temperature noise suppression technology based on feedback correction phase-shift compensation algorithm has been developed, significantly reducing the impact of long-period disturbances [239, 240, 241, 242, 243]. Combining the above two technologies, a

high-precision temperature controller has been developed, and the principle prototype design have been completed.

According to the overall satellite configuration and thermal design plan, a high thermal resistance and high thermal capacity structure is used under the solar cell array to attenuate and isolate the space thermal flow. With the technology to create high-gel-activity sol, two types of thermal insulation materials with high strength and low modulus and ultra-low thermal conductivity have been prepared. The thermal insulation material with thermal conductivity $< 0.03 \text{ W}/(\text{m}\cdot\text{K})$ has been developed [244, 245].

For design verification, the test schemes for the scale model and the fast response model have been determined, and the simulation method corresponding to the satellite's external heat flow has been formulated, through the equivalent simulation technology with frequency-domain discretization of temperature boundary and heat flow boundary [246], and by formulating the sinusoidal amplitude response curve based on the transfer function. The preliminary design of the corresponding tests has been completed.

4. Developing Key Technologies for TianQin

Coordinator: Zebing Zhou, Hsien-Chi Yeh, Chao Xue

In this section we report the progress on the two key technologies of the TianQin project: the inertial reference technology and the inter-satellite laser interferometry technology.

4.1. Inertial reference

Coordinator: Zebing Zhou

In the context of space-based GW detection, the inertial reference is of paramount importance. The system is comprised of three fundamental components: the inertial sensor is meticulously engineered to minimize TM disturbances through components such as the sensitive head and sensing/control systems; the micro-Newton thrusters are developed to counteract non-conservative forces acting on the satellite platform; drag-free control is achieved through dynamic modeling, diverse control algorithms, and ground simulation experiments, ensuring precise satellite and TM motion control. These elements collectively contribute to the success of the detection mission.

4.1.1. Inertial sensor

Coordinator: Yanchong Liu

Based on functions and disturbance suppression requirements, inertial sensors are mainly composed of the sensitive head, sensing and control system, charge management system, caging and releasing system, vacuum maintenance system. For the space-based GW detection, the TM is the inertial reference and provides a reference point for laser interferometry. TianQin requires the residual acceleration of the TMs along the sensitive axis to be less than $1 \times 10^{-15} \text{ m/s}^2/\text{Hz}^{1/2}$ [13].

Sensitive head The sensitive head is the core of the inertial sensor, which is composed of TM, electrode plate and electrode housing. The TM must have high density, superior thermal conductivity, low remanence, and low magnetic susceptibility to minimize disturbances. In TianQin, the TM is a cubic gold-platinum alloy with a

mass of about 2.5 kg. Considering the low disturbance requirement of the sensitive axis and carrier injection requirement, the plate configuration scheme of three-axis control plate and two-non-sensitive axis injection plate will be used for TianQin. The electrode housing is responsible for carrying the plate and providing the necessary electromechanical interface for the other system.

Prototypes of the TM and electrode housing have been created. The TM exhibited excellent magnetic performance, with a susceptibility of 8×10^{-6} and a residual magnetic moment of approximately $10 \text{ nA} \cdot \text{m}^2$, meeting the requirement of TianQin [247].

Sensing and control system The sensing and control system mainly includes capacitance sensing unit, electrostatic control unit and control unit. The capacitive sensing unit and electrostatic control unit are used for the measurement and control of the six degrees of freedom motion of the TM. For TianQin, the requirement for capacitance sensing is $7 \times 10^{-7} \text{ pF/Hz}^{1/2}$ at 6 mHz. A prototype of the capacitive sensing unit has been created with a resolution of $2.3 \times 10^{-7} \text{ pF/Hz}^{1/2}$, mainly limited by thermal noise from the transformer and pre-amplifier [248, 249, 250, 251, 252]. A prototype of the electrostatic control unit has been realized with a voltage noise of $1 \times 10^{-5} \text{ V/Hz}^{1/2}$, meeting the requirement of TianQin.

Charge management system The charge management system is responsible for measuring the TM's residual charge and using ultraviolet discharge technology to neutralize the residual charge resulting from high-energy charged particle collisions on the TM. A 254 nm Micro-LED with power exceeding $3 \times 10^{-6} \text{ W}$ has been developed, with a measured lifetime exceeding 5000 h. An engineering model for the charge management subsystem has been developed, with a charging rate capability of $5 \times 10^5 \text{ e/s}$ [253, 254, 255, 249, 256]. A ground test and verification of the charge management system using a torsion pendulum was constructed, achieving a charge control level of $6.6 \times 10^{-14} \text{ C}$, which is almost an order of magnitude better than the requirement ($3.4 \times 10^{-13} \text{ C}$).

TM Lock and release system Due to the substantial mass of the TM and its considerable separation from the electrode frame, the unconstrained TM will possess destructive kinetic energy during the launch phase. Therefore, to ensure the safe transition of the inertial sensors into the scientific operational mode, a dedicated lock and release system is necessary, taking into account the launch conditions and release requirements [257]. The system is designed to fully lock the TM during the launch phase, release it with near-zero initial velocity to a free-falling state, and subsequently capture it using an electrostatic actuator. The design of the lock and release system has been finalized, and a prototype of the principle has been developed. Preliminary test of the system's locking, capturing, positioning and releasing functions has been completed [258]. The lock force of the system has been determined to exceed 1500 N, and the transferred momentum and angular momentum have been estimated at the level 10^{-5} kg m/s and $10^{-7} \text{ kg m}^2/\text{s}$, respectively.

System integration and ground testing A preliminary design of inertial sensor system integration for TianQin has been completed, with titanium vacuum chamber developed, probe and vacuum chamber installed together, and caging and release

subsystem tested. The integrated inertial sensor flight model is planned to be tested with the TianQin-2 satellite.

Regarding disturbance investigation, high precision torsion pendulum has been used to investigate patch effect [259], magnetic effect [260, 261], thermal gradient effect [262], and gas damping effect [263] thus far. The experimental results are in agreement with the theoretical analysis. Design and requirements of the inertial sensor are iteratively revised based on theoretical analysis and experimental results.

4.1.2. Micro-Newton thruster

Coordinator: Peiyi Song, Jianping Liu, Yong Li

As the actuator of the DFC system, the micro-Newton thruster is a key component and the performance of the micro-Newton thruster constrains the level of DFC largely. TianQin mandates high requirements for micro-Newton thrusters, including continuously adjustable thrust between 0-100 μN , resolution of $<0.1 \mu\text{N}$, and thrust noise of $<0.1 \mu\text{N}/\text{Hz}^{1/2}$ [264].

Cold gas micro-Newton thrusters offer ultra fine precision and superior reliability. The cold gas micro-Newton thrusters used in GW detection require three key technologies: micro-Newton piezoelectric thruster, microgram gas flowsensor and low noise thrust control. The controller converts commanded thrust to flow rate according to on-ground calibrated formula, then the piezoelectric thruster adjusts the throat area of the proportional piezoelectric valve based on the feedback value of the gas flowsensor. This converges the gas flow rate to the setting point, thereby achieving closed-loop control of thrust. In order to match gas flow rate to thrust, the gas flowsensor must be as close as possible to the piezoelectric valve and integrated inside cold gas micro-Newton thrusters. [265, 266, 267].

The performance of the cold gas micro-Newton thruster relies on high-precision piezoelectric-driven flow control method. Piezoelectric-driven elements in the cold gas micro-Newton thruster utilize the inverse piezoelectric effect to convert electrical energy into mechanical energy, which is then transmitted through a specific structure to achieve fluid control and regulation. Due to the characteristics of high precision, high resolution, low power consumption, low electromagnetic interference, and relatively mature technology, piezoelectric-driven valves have a broad application prospect in the field of high-precision fluid control and have become the preferred solution for the cold gas micro-Newton thruster of space-based GW detection missions [268, 269].

Due to the extremely low thrust of cold gas micro-Newton thrusters, they are highly susceptible to the flow characteristics of the propellant and the flow related disturbances, making it difficult to achieve high-precision and stable thrust output through open-loop control. It is necessary to establish an accurate thrust model and closed-loop thrust control methods. The flow sensor acts as the reference signal for thrust control, with its flow measurement resolution setting the upper threshold for thrust control performance. Employing a thermal flow sensing solution, the flowsensor leverages the advantage of temperature differential measurement to mitigate environmental interferences. [270].

Targeting the need of the TianQin project, research on micro-Newton cold gas thrust control technology has been carried out and in-orbit verification has been achieved with the TianQin-1 satellite. The micro-Newton gas thruster carried by TianQin-1 has a thrust resolution of approximately $0.1 \mu\text{N}$. The in-orbit experimental measurements show that the thrust can be precisely adjusted from 1 to $60 \mu\text{N}$. For

periods where the output of the micro-Newton thruster remains constant, the overall thrust noise is $0.3 \mu\text{N}/\text{Hz}^{1/2}$ at 0.1 Hz [271].

The construction of the micro-Newton gas propulsion system for the TianQin-2 is being carried out as planned. It consists of a gas bottle, a gas addition and exhaust valve, a self-locking valve, a high-pressure pressure sensor, a low-pressure pressure sensor, a filter, a micro-Newton variable thrust module, a circuit box, and piping components. The expected thrust range is 0.1 to 1000 μN .

4.1.3. Drag-free control

Coordinator: Guoying Zhao, Xingyu Gou

In this subsection, the current status of DFC technology in the TianQin project is briefly summarised from the following three perspectives: dynamic modelling, control algorithms, and ground simulation experiments.

Dynamic modelling The main objective of the dynamic modelling is to obtain mathematical models that describe the motion coupling between the satellite, the optomechanical assembly and the TMs. In addition, it is a fundamental step to derive linearised and decoupled models and to develop suitable controllers.

The Drag-Free Attitude Control System (DFACS) can be divided into three main phases after the S/C reaching orbit: releasing TM, constellation acquisition, and scientific mode. The interaction between the S/C attitude, laser pointing, and TM leads to complex multi-degree-of-freedom control across multiple modes. In addition, the core payload is currently in the phase of being systematised. It is therefore necessary to investigate the impact of different system configurations on the control system. These requirements demand a sufficient understanding of the S/C dynamics model.

At present stage, a dynamic model has been developed that can completely describes the kinematics of the motion coupling. Compared to other models, this model does not have restrictive assumptions (e.g. kinematic states and system parameter configurations). The accuracy of the dynamic model has been verified by comparing it with the Simscape model. The results show that the model has higher accuracy than the existing model in all degrees of freedom. Monte Carlo simulations have been performed using random parameters to demonstrate that the model can be used for different parameter configurations and three different stages of the DFACS. What's more, a corresponding simplified model in scientific mode is proposed based on the orbital configuration of the TianQin S/C. The simplified model greatly reduces the system complexity while maintaining the main system dynamics, and therefore can further improve the efficiency of control design in scientific mode. In summary, the obstacles of the DFACS in modeling the dynamics of S/C have been removed. More detailed information about the dynamic model can be found in [215].

Control algorithm Control algorithms are the core of DFACS. A variety of control algorithms have been developed now.

A simple single integral controller has been implemented for the acceleration-mode DFC on TianQin-1, focusing on solving practical engineering problems and achieving stable, reliable, and highly repeatable control results [272]. For DFC in general, the displacement-mode DFC feasibility and thrust saturation avoidance has been explored [273], adaptive control theories, proposing adaptive methods, and designing estimation

and control strategies have been developed [274, 275, 276, 277]. A new design strategy has been proposed for the Drag-Free S/C, which effectively solves the frequency band limitation of the control signal in the scientific mode through frequency separation theory, while reducing fuel consumption [278]. A multi-loop controller design method has been proposed for the Drag-Free S/C, which effectively improves the design efficiency by transforming the performance index into frequency domain constraints and using a multi-group genetic algorithm to optimize the controller design [279]. A model predictive control method has been proposed to solve the fault-tolerant control problem of a Drag-Free S/C under actuator faults and input saturation [280]. An embedded model control (EMC) structure has been designed based on a decoupled dynamic model and used a loop shaping method to adjust the controller parameters [281]. The proposed controller design was verified by numerical simulation. The results show that the fluctuation of the relative displacement of the TM is controlled below $3 \text{ nm/Hz}^{1/2}$, which meets the requirements of TianQin. In addition, Monte Carlo experiments show that the dynamic performance of the closed loop is only slightly affected by parameter uncertainties, demonstrating the robustness of the EMC. A proportional-integral-derivative feedforward controller has been designed for TianQin-1 and implemented it in the FPGA chip of the electrostatic accelerometer [282]. The performance of the DFC system was verified through in-orbit experiments. The results show that a residual acceleration of $5 \times 10^{-11} \text{ m/s}^2/\text{Hz}^{1/2}$ at 10 mHz was achieved.

Current research results on control algorithms focus mainly on scientific models and neglect the degrees of freedom of the optomechanical assemblies. Control design that considers the complete degrees of freedom and other modes in addition to scientific modes is currently ongoing. For more detailed information on control design, please refer to the references [215, 272, 273, 274, 275, 276, 277, 275, 278, 279, 280, 281, 282].

Ground simulation experiments Given the high cost and significant risk of direct in-orbit testing of the DFC system, ground-based simulation and validation are essential.

A high-precision satellite simulator designed to validate inter-satellite laser tracking performance has been developed. An air-bearing system is employed to minimize friction and torque between the simulator and the underlying surface. The satellite platform is equipped with four sets of orthogonally mounted gas thrusters, which can be combined to generate the desired forces and torques for the satellite platform. The satellite platform performs coarse laser tracking, while an optical platform is used for fine laser tracking.

The developed EMC algorithm has been applied to this satellite simulator. Results indicate that the satellite platform achieves measurement tracking errors of better than $10 \text{ mrad/Hz}^{1/2}$ during fixed-position tracking and better than $50 \text{ mrad/Hz}^{1/2}$ during motion tracking. The optical platform reduces measurement tracking errors to $80 \text{ } \mu\text{rad/Hz}^{1/2}$. This simulator demonstrates potential for simulating laser tracking missions. More detailed information about the satellite simulator can be found in [282].

TianQin is also currently constructing some other ground simulation facilities that can be used for Drag-Free verification.

4.2. Intersatellite laser interferometry

Coordinator: Hsien-Chi Yeh

The inter-satellite laser interferometry system is the core payload system for measuring the optical-path-length changes caused by the GWs. So far, all proposed space-based GW detection missions are based on three-satellite constellation with six inter-satellite laser links. Due to a very weak light power received by the remote satellite after propagating through a large inter-satellite distance, a transponder-type interferometer, instead of a typical Michelson's interferometer, must be used for inter-satellite laser interferometry.

A simplified configuration of inter-satellite transponder laser interferometer consists of a frequency-stabilized laser, ultra-stable optical benches, weak-light phase locking control unit, and telescopes that can be treated as laser couplers to the ultra-stable optical benches. In TianQin-1 mission, we have tested the performances of ultra-stable optical bench and phasemeter. The noise level of laser interferometer achieved $30 \text{ pm/Hz}^{1/2}$ @ 0.1 Hz. In TianQin-2 mission, planned to be launched around 2026, a complete inter-satellite transponder laser interferometer will be demonstrated. Besides ultra-stable optical benches and phasemeters, a frequency-stabilized laser unit and a weak-light phase locking control unit will be demonstrated in orbit.

In the following, we present the current progress on developing the frequency-stabilized laser, the ultra-stable optical benches, the weak-light phase locking control unit and the telescope.

4.2.1. Frequency stabilized Laser

The laser source is based on a master oscillator power amplifier architecture, and the output frequency is stabilized by the frequency stabilization unit (FSU). There are three main parts: the seed laser, the optical amplifier and FSU.

The seed laser is a Nd:YAG nonplanar ring cavity solid-state laser pumped by 808-nm laser diodes [283, 284], which has two tuning channels, the piezoelectric tuning channel and the temperature tuning channel, to realize the functions of frequency stabilization and phase locking. The free-space light generated by the pump diode is focused into the Nd:YAG crystal through coupling lens, and the output 1064-nm free-space laser is linearly polarized by wave-plates and then injected into a single-mode polarization maintaining fiber through a fiber coupler. In order to improve the reliability of the seed laser, two pump diodes are packaged into the seed laser, while under nominal condition, only one pump diode is working and the other is the offline backup.

The optical amplifier is based on a Yb-doped fiber amplifier architecture, which can output watt-level linear-polarized laser at 1064-nm wavelength [285]. The seed laser and a 976-nm pump laser are injected into the double-cladding active fiber through a fiber coupler. The fiber mode field adapters and fiber isolators are used to adjust the mode size in the fiber and to protect the seed laser. In the end of the fiber optical link, fiber splitters are used to realize power stabilization feedback and power monitoring, while the port on the main path outputs watt-level laser for inter-satellite laser interferometry. Multiple pump diodes are packaged in the optical fiber amplifier to improve the reliability and to compensate for potential laser power degradation during the operation period in space.

The FSU adopts the integrated quasi-monolithic ultra-stable optical resonator made by using hydroxide-catalysis bonding technique [286, 287], and the laser frequency locking is realized with the Pound-Drever-Hall scheme. The FSU use all-fiber optical link and FPGA-based digital feedback controller that performs the frequency locking to the resonance frequency of the ultra-stable cavity. The measured

frequency noise spectral density is about $30 \text{ Hz/Hz}^{1/2}$ at Fourier frequencies from 10 mHz to 1 Hz. When testing the frequency noise, the prototype is actively suppressed from vibration noise on the ground, and uses active temperature control to ensure that its temperature is near the zero-expansion-point of the ultra-stable cavity. The prototype is compared with another set of independent ultra-stable cavity FSU (same active vibration isolation with the active temperature control at zero-expansion-point), where the beat frequency is measured by a frequency counter.

The three main parts of laser source (seed laser, optical amplifier and FSU) are independently designed and packaged. The prototypes of the three units have passed typical space-compatibility tests, including random and periodic vibrations, impact, thermal cycles, etc. In the next step, it is necessary to carry out the integrated design among the three units under full consideration of the space environment adaptability. In addition, in order to realize clock comparison and pseudo-random-code ranging, an optical modulation module will be added to the integrated design. The laser power stabilization unit is also under development.

4.2.2. Optical bench

The optical bench is a core payload of the laser interferometer system used in space-based GW detection missions. The design, engineering fabrication, noise analysis and suppression of optical benches are the focus of the state-of-the-art researches [288, 289, 290, 291, 292]. For TianQin, the ultra-stable optical bench and FPGA-based phasemeter have been demonstrated in TianQin-1 mission [271, 293], reaching the noise level $10 \text{ nm/Hz}^{1/2}$ @ 6 mHz and up to $100 \text{ nm/Hz}^{1/2}$ @ 1 mHz. For the measurement noise of interferometer at frequency range of $0.1 \text{ Hz} \sim 1 \text{ mHz}$, it has been investigated and found that the stray lights reflected from the optical components of the optical bench is one of the major error sources.

The stray light occurred on the optical bench is equivalent to an additional reference laser beam that also generates an interference signal when beating with the received weak light, and then provides an additional phase into the total phase difference measured. The theoretical model reveals that this stray light effect of the optical bench results in a nonlinear error, periodically varying with the optical path length (OPL). Base on the periodic property of this nonlinear optical-path-length error, a proper optical path length can be chosen as the initial measuring position of laser interferometer so that the nonlinear error is minimized, hence the stray light effect can be negligible [294].

A Mach-Zehnder interferometer system has been built to test the theoretical model and the feasibility of the error suppression method. Fig. 3 shows the experimental setup. A heterodyne frequency between two laser beams is generated by two acousto-optic modulators (AOM1 and AOM2). The modulated laser beams are guided into a Mach-Zehnder interferometer that is made with silicate bonding technique. In order to adjust the OPL of the reference beam of interferometer, a PZT-driven mirror, M2, is installed in the optical path of the upper laser beam. Two interference signals are detected by photodetectors, PDM and PDR, and then are sent to phasemeter by which the phase difference between two laser beams can be acquired. To verify the periodic property of the nonlinear error caused by the stray light, the OPL of the reference beam is increased linearly by using PZT-driven mirror. The peak-to-peak value of the nonlinear error has been found to be 0.26 nm [294].

Regarding the laser interferometer for TianQin-2 mission, the prototype of the optical bench had been constructed and accomplished space-compatibility tests, like

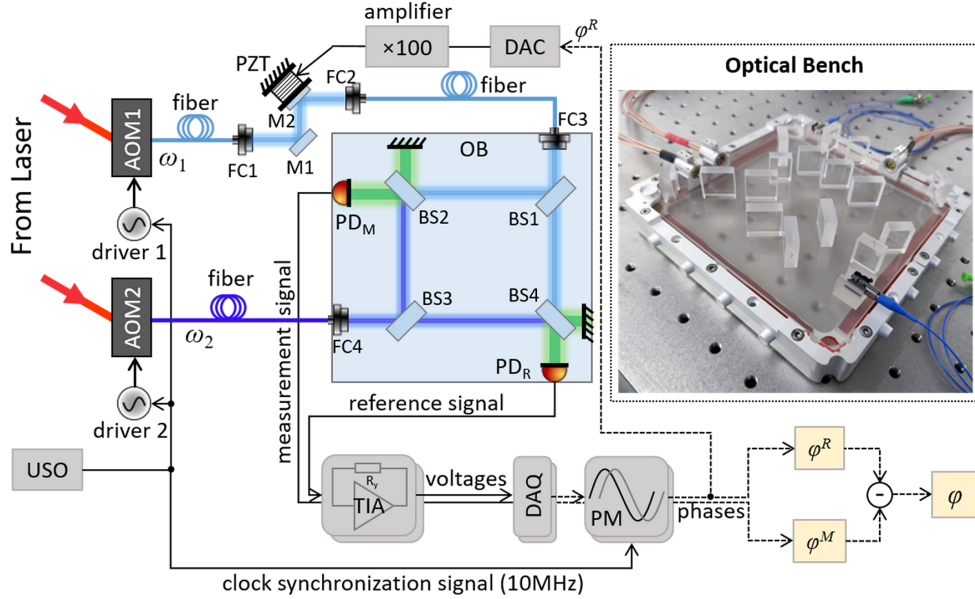


Figure 3. Experimental setup of an OPL-tunable heterodyne Mach-Zehnder interferometer [294]. USO: ultra-stable oscillator; FC: fiber collimator; BS: beam splitter; TIA: trans-impedance amplifier; DAQ: data acquisition device; PM: phasemeter.

periodic vibrations, random vibrations and thermal cycle tests. The ground-based experiment shows that the noise level of the optical bench achieved $2 \text{ pm/Hz}^{1/2}$ @ 0.1 Hz and $6 \text{ pm/Hz}^{1/2}$ @ 10 mHz .

4.2.3. Phasemeter and weak-light phase locking

The phasemeter for TianQin is being developed and has achieved a very high precision. The current research has revealed that the measurement error of phasemeter is mainly caused by the phase sampling jitter that is closely related to the devices of analog-to-digital converter (ADC) and ultra-stable oscillator. The former converts interference beat signal to digital signal, and the latter provides trigger signals to phasemeter and optical phase-locked loop. The noises caused by the sampling jitter of ADC and the noise of ultra-stable oscillator can be reduced by using the pilot-tone correction and the inter-satellite side-band modulation techniques, respectively. However, the low-frequency ($0.1 \text{ mHz} \sim 0.1 \text{ Hz}$) noise of the phasemeter and weak-light phase locking control is still a challenging problem.

For low frequency noises of phasemeter, the major noise sources of phasemeter include thermal fluctuation of temperature-sensitive electrical device [295], inter-channel cross talk [295, 296], and quantization error of numerical control oscillator [297]. We focus on discussion about the thermal fluctuation of temperature-sensitive electrical device in the following.

The phasemeter unit consists of a lot of analog and digital components and devices. For analog components, like resistances and capacitances, their transfer functions can be obtained without much difficulty. For more complicated devices, e.g.

ADC and multiplexers, it's difficult to build up proper theoretical models for analyzing their thermal characteristics. In this case, we apply temperature modulation to these complicated devices in order to calibrate the temperature coefficients [298]. Using such experiment, we can evaluate the thermal characteristics of temperature-sensitive components and devices used in the phasemeter and weak-light phase-locked loop. Accordingly, we can determine the upper limits of temperature variations allowed for these temperature-sensitive components and devices.

4.2.4. Telescope

Coordinator: Lei Fan

Telescope is another core payload of the laser interferometer system. It functions as an afocal beam expander and operates simultaneously in transmit and receive modes. Its primary purpose is to facilitate a precise length measurement between the optical benches (and ultimately the TMs) on widely separated S/C.

The optical design for TianQin telescope adopts the off-axis quad-mirror optical structure. It takes a collimated beam from the optical bench, with a diameter of approximately 4 mm and transforms it into a collimated beam, with a diameter of about 300 mm, and a profile optimized to deliver power efficiently on-axis in the far field. The latest design shows that the telescope has a magnification of 75, with M1 being parabolic, M2 hyperbolic, M3 a folding mirror, and M4 a freeform surface. Within the ± 30 μ rad science field of view, wave front errors are better than RMS 0.0074λ ($\lambda=1064\text{nm}$). Optical system design schemes where both M3 and M4 are freeform surfaces have also been attempted. Although higher specifications can be achieved in the design, the difficulty of manufacturing and alignment increases dramatically. Therefore, they have not been chosen for prototype engineering. The tolerance budget guarantees that there is over a 90% probability that the telescope's wave front error will be better than RMS 25 nm. The spatial distances between M1 through M4 have been fully considered for compactness, structural support, alignment, and assembly requirements. To fulfill the stability requirements, both the mirrors and supporting structures are made from low expansion glass, mainly due to its ultra-low coefficient of thermal expansion, ease of welding and bonding. Under the premise of relaxing the wave front aberration, methods such as controlling the coupling aberration proportion and optimizing the beam waist radius have been proposed to suppress the non-geometric TTL coupling noise [299, 300, 301]. In terms of coating, it has been found that metal coatings can effectively suppress the optical path noise caused by low-frequency temperature fluctuations [302].

The optical path length stability of the telescope is a key technical indicator for the space-based GW detection. In the observation band from 0.1 mHz to 1 Hz, the telescope must exhibit an optical path length stability of $0.4 \text{ pm/Hz}^{1/2}$. We designed a detection scheme based on Pound-Drever-Hall technology and analyzed its noise requirement level [303]. Furthermore, an analysis indicates that when the detected telescope wave front aberration is better than 0.068λ ($\lambda=1064 \text{ nm}$) with a probability of 98%, the coupling efficiency of the off-axis resonant cavity can exceed 40% [304].

5. Summary

The TianQin project aims to launch the space-based GW detector, TianQin, around 2035. The project has been progressing smoothly following the "0123" technology roadmap. After the success of step "0" and step "1" missions, which have

demonstrated the high orbit satellite laser ranging and the DFC technology for TianQin, the step “2” mission has been officially approved in 2021 and is expected to test the inter-satellite laser interferometry technology for TianQin using a pair of satellites in a couple of years. Researches surrounding the final step, the construction and the launch of the GW detection satellites, are also moving forward as expected.

Acknowledgments

The work has been supported in part by the National Key Research and Development Program of China (Grant No. 2020YFC2200200, 2020YFC2200500, 2022YFC2204000, 2022YFC2204200, 2023YFC2206700), the Guangdong Major Project of Basic and Applied Basic Research (Grant No. 2019B030302001), the National Natural Science Foundation of China (Grants No. 12261131504, 11927812), the Basic and Applied Basic Research Foundation of Guangdong Province (Grant Number 2024A1515010142), the 111 Project (Grant No.B20062), and the Fundamental Research Funds for the Central Universities, Sun Yat-sen University. The work of VM and KP is supported by Russian Science Foundation grant No 23-42-00055.

References

- [1] B. P. Abbott et al. Observation of Gravitational Waves from a Binary Black Hole Merger. *Phys. Rev. Lett.*, 116(6):061102, 2016.
- [2] Matthew Evans et al. A Horizon Study for Cosmic Explorer: Science, Observatories, and Community. 9 2021.
- [3] Michele Maggiore et al. Science Case for the Einstein Telescope. *JCAP*, 03:050, 2020.
- [4] Marica Branchesi et al. Science with the Einstein Telescope: a comparison of different designs. *JCAP*, 07:068, 2023.
- [5] Heng Xu et al. Searching for the Nano-Hertz Stochastic Gravitational Wave Background with the Chinese Pulsar Timing Array Data Release I. *Res. Astron. Astrophys.*, 23(7):075024, 2023.
- [6] J. Antoniadis et al. The second data release from the European Pulsar Timing Array - III. Search for gravitational wave signals. *Astron. Astrophys.*, 678:A50, 2023.
- [7] Daniel J. Reardon et al. Search for an Isotropic Gravitational-wave Background with the Parkes Pulsar Timing Array. *Astrophys. J. Lett.*, 951(1):L6, 2023.
- [8] Gabriella Agazie et al. The NANOGrav 15 yr Data Set: Evidence for a Gravitational-wave Background. *Astrophys. J. Lett.*, 951(1):L8, 2023.
- [9] M. Falxa et al. Searching for continuous Gravitational Waves in the second data release of the International Pulsar Timing Array. *Mon. Not. Roy. Astron. Soc.*, 521(4):5077–5086, 2023.
- [10] P. A. R. Ade et al. Improved Constraints on Primordial Gravitational Waves using Planck, WMAP, and BICEP/Keck Observations through the 2018 Observing Season. *Phys. Rev. Lett.*, 127(15):151301, 2021.
- [11] Hong Li et al. Probing Primordial Gravitational Waves: Ali CMB Polarization Telescope. *Natl. Sci. Rev.*, 6(1):145–154, 2019.
- [12] Pau Amaro-Seoane et al. Laser Interferometer Space Antenna. 2 2017.
- [13] Jun Luo et al. TianQin: a space-borne gravitational wave detector. *Class. Quant. Grav.*, 33(3):035010, 2016.
- [14] Jianwei Mei et al. The TianQin project: current progress on science and technology. *PTEP*, 2021(5):05A107, 2021.
- [15] Wen-Rui Hu and Yue-Liang Wu. The Taiji Program in Space for gravitational wave physics and the nature of gravity. *Natl. Sci. Rev.*, 4(5):685–686, 2017.
- [16] Yungui Gong, Jun Luo, and Bin Wang. Concepts and status of Chinese space gravitational wave detection projects. *Nature Astron.*, 5(9):881–889, 2021.
- [17] Seiji Kawamura et al. Current status of space gravitational wave antenna DECIGO and B-DECIGO. *PTEP*, 2021(5):05A105, 2021.
- [18] Shun-Jia Huang, Yi-Ming Hu, Valeriya Korol, Peng-Cheng Li, Zheng-Cheng Liang, Yang Lu, Hai-Tian Wang, Shenghua Yu, and Jianwei Mei. Science with the TianQin Observatory:

- Preliminary results on Galactic double white dwarf binaries. *Phys. Rev. D*, 102(6):063021, 2020.
- [19] Shuai Liu, Yi-Ming Hu, Jian-dong Zhang, and Jianwei Mei. Science with the TianQin observatory: Preliminary results on stellar-mass binary black holes. *Phys. Rev. D*, 101(10):103027, 2020.
- [20] Hui-Min Fan, Yi-Ming Hu, Enrico Barausse, Alberto Sesana, Jian-dong Zhang, Xuefeng Zhang, Tie-Guang Zi, and Jianwei Mei. Science with the TianQin observatory: Preliminary result on extreme-mass-ratio inspirals. *Phys. Rev. D*, 102(6):063016, 2020.
- [21] Hai-Tian Wang et al. Science with the TianQin observatory: Preliminary results on massive black hole binaries. *Phys. Rev. D*, 100(4):043003, 2019.
- [22] Zheng-Cheng Liang, Yi-Ming Hu, Yun Jiang, Jun Cheng, Jian-dong Zhang, and Jianwei Mei. Science with the TianQin Observatory: Preliminary results on stochastic gravitational-wave background. *Phys. Rev. D*, 105(2):022001, 2022.
- [23] En-Kun Li et al. Gravitational Wave Astronomy With TianQin. 9 2024.
- [24] Jun Luo et al. Fundamental Physics and Cosmology with TianQin, in preparation.
- [25] Alejandro Torres-Orjuela, Shun-Jia Huang, Zheng-Cheng Liang, Shuai Liu, Hai-Tian Wang, Chang-Qing Ye, Yi-Ming Hu, and Jianwei Mei. Detection of astrophysical gravitational wave sources by TianQin and LISA. *Sci. China Phys. Mech. Astron.*, 67(5):259511, 2024.
- [26] Alexander Stroer and A. Vecchio. The LISA verification binaries. *Class. Quant. Grav.*, 23:S809–S818, 2006.
- [27] Shuai Liu, Liang-Gui Zhu, Yi-Ming Hu, Jian-dong Zhang, and Mu-Jie Ji. Capability for detection of GW190521-like binary black holes with TianQin. *Phys. Rev. D*, 105(2):023019, 2022.
- [28] Hui-Min Fan, Shiyan Zhong, Zheng-Cheng Liang, Zheng Wu, Jian-dong Zhang, and Yi-Ming Hu. Extreme-mass-ratio burst detection with TianQin. *Phys. Rev. D*, 106(12):124028, 2022.
- [29] Changfu Shi, Xinyi Che, Zeyu Huang, Yi-Ming Hu, and Jianwei Mei. Gravitational waves and cosmic boundary. *Phys. Rev. D*, 111(2):023022, 2025.
- [30] Zijian Wang, Zhoujian Cao, and Xian-Fei Zhang. Measuring mass transfer of AM CVn binaries with a space-based gravitational wave detector. *Mon. Not. Roy. Astron. Soc.*, 525(1):270–278, 2023.
- [31] Thomas Kupfer et al. LISA Galactic Binaries with Astrometry from Gaia DR3. *Astrophys. J.*, 963(2):100, 2024.
- [32] Kaitlyn Szekerczes, Scott Noble, Cecilia Chirenti, and James Ira Thorpe. Imaging the Milky Way with Millihertz Gravitational Waves. *Astron. J.*, 166(1):17, 2023.
- [33] Yong Shao and Xiang-Dong Li. Population Synthesis of Black Hole Binaries with Compact Star Companions. *Astrophys. J.*, 920(2):81, 2021.
- [34] Alexandre Toubiana et al. Detectable environmental effects in GW190521-like black-hole binaries with LISA. *Phys. Rev. Lett.*, 126(10):101105, 2021.
- [35] Laura Sberna et al. Observing GW190521-like binary black holes and their environment with LISA. *Phys. Rev. D*, 106(6):064056, 2022.
- [36] Han Wang, Ian Harry, Alexander Nitz, and Yi-Ming Hu. Space-based gravitational wave observatories will be able to use eccentricity to unveil stellar-mass binary black hole formation. *Phys. Rev. D*, 109(6):063029, 2024.
- [37] Yuya Sakurai, Naoki Yoshida, Michiko S. Fujii, and Shingo Hirano. Formation of Intermediate-Mass Black Holes through Runaway Collisions in the First Star Clusters. *Mon. Not. Roy. Astron. Soc.*, 472(2):1677–1684, 2017.
- [38] Lorenz Zwick, Christopher Tiede, Alessandro A. Trani, Andrea Derdzinski, Zoltan Haiman, Daniel J. D’Orazio, and Johan Samsing. Novel category of environmental effects on gravitational waves from binaries perturbed by periodic forces. *Phys. Rev. D*, 110(10):103005, 2024.
- [39] Bin Liu and Dong Lai. Probing the Spins of Supermassive Black Holes with Gravitational Waves from Surrounding Compact Binaries. *Astrophys. J.*, 924(2):127, 2022.
- [40] Amy Secunda, Jillian Bellovary, Mordecai-Mark Mac Low, K. E. Saavik Ford, Barry McKernan, Nathan Leigh, Wladimir Lyra, and Zsolt Sándor. Orbital Migration of Interacting Stellar Mass Black Holes in Disks around Supermassive Black Holes. *Astrophys. J.*, 878(2):85, 2019.
- [41] Amy Secunda, Jillian Bellovary, Mordecai-Mark Mac Low, K. E. Saavik Ford, Barry McKernan, Nathan W. C. Leigh, Wladimir Lyra, Zsolt Sandor, and Jose I. Adorno. Orbital Migration of Interacting Stellar Mass Black Holes in Disks around Supermassive Black Holes II. Spins and Incoming Objects. *Astrophys. J.*, 903(2):133, 2020.
- [42] J. Samsing, I. Bartos, D. J. D’Orazio, Z. Haiman, B. Kocsis, N. W. C. Leigh, B. Liu, M. E. Pessah, and H. Tagawa. AGN as potential factories for eccentric black hole mergers. *Nature*,

- 603(7900):237–240, 2022.
- [43] Qianhang Ding, Tomohiro Nakama, Joseph Silk, and Yi Wang. Detectability of Gravitational Waves from the Coalescence of Massive Primordial Black Holes with Initial Clustering. *Phys. Rev. D*, 100(10):103003, 2019.
- [44] Lorenz Zwick, Lucio Mayer, Lionel Haemmerlé, and Ralf S. Klessen. Direct collapse of exceptionally heavy black holes in the merger-driven scenario. *Mon. Not. Roy. Astron. Soc.*, 518(2):2076–2087, 2022.
- [45] Hong-Yu Chen, Xiang-Yu Lyu, En-Kun Li, and Yi-Ming Hu. Near real-time gravitational wave data analysis of the massive black hole binary with TianQin. *Sci. China Phys. Mech. Astron.*, 67(7):279512, 2024.
- [46] Pau Amaro-Seoane. Detecting Intermediate-Mass Ratio Inspirals From The Ground And Space. *Phys. Rev. D*, 98(6):063018, 2018.
- [47] Manuel Arca-Sedda, Pau Amaro-Seoane, and Xian Chen. Merging stellar and intermediate-mass black holes in dense clusters: implications for LIGO, LISA, and the next generation of gravitational wave detectors. *Astron. Astrophys.*, 652:A54, 2021.
- [48] Alejandro Torres-Orjuela, Xian Chen, and Pau Amaro Seoane. Excitation of gravitational wave modes by a center-of-mass velocity of the source. *Phys. Rev. D*, 104(12):123025, 2021.
- [49] Alejandro Torres-Orjuela, Pau Amaro Seoane, Zeyuan Xuan, Alvin J. K. Chua, María J. B. Rosell, and Xian Chen. Exciting Modes due to the Aberration of Gravitational Waves: Measurability for Extreme-Mass-Ratio Inspirals. *Phys. Rev. Lett.*, 127(4):041102, 2021.
- [50] Nicolas Yunes, Bence Kocsis, Abraham Loeb, and Zoltan Haiman. Imprint of Accretion Disk-Induced Migration on Gravitational Waves from Extreme Mass Ratio Inspirals. *Phys. Rev. Lett.*, 107:171103, 2011.
- [51] Enrico Barausse, Vitor Cardoso, and Paolo Pani. Can environmental effects spoil precision gravitational-wave astrophysics? *Phys. Rev. D*, 89(10):104059, 2014.
- [52] Mudit Garg, Andrea Derdzinski, Lorenz Zwick, Pedro R. Capelo, and Lucio Mayer. The imprint of gas on gravitational waves from LISA intermediate-mass black hole binaries. *Mon. Not. Roy. Astron. Soc.*, 517(1):1339–1354, 2022.
- [53] Hugo Pfister, Martina Toscani, Thomas Hong Tsun Wong, Jane Lixin Dai, Giuseppe Lodato, and Elena M. Rossi. Observable gravitational waves from tidal disruption events and their electromagnetic counterpart. *Mon. Not. Roy. Astron. Soc.*, 510(2):2025–2040, 2022.
- [54] Chang-Qing Ye, Jin-Hong Chen, Jian-dong Zhang, Hui-Min Fan, and Yi-Ming Hu. Observing white dwarf tidal stripping with TianQin gravitational wave observatory. *Mon. Not. Roy. Astron. Soc.*, 527(2):2756–2764, 2023.
- [55] Clifford M. Will. The Confrontation between General Relativity and Experiment. *Living Rev. Rel.*, 17:4, 2014.
- [56] B. P. Abbott et al. Tests of general relativity with GW150914. *Phys. Rev. Lett.*, 116(22):221101, 2016. [Erratum: Phys.Rev.Lett. 121, 129902 (2018)].
- [57] B. P. Abbott et al. Tests of General Relativity with the Binary Black Hole Signals from the LIGO-Virgo Catalog GWTC-1. *Phys. Rev. D*, 100(10):104036, 2019.
- [58] R. Abbott et al. Tests of general relativity with binary black holes from the second LIGO-Virgo gravitational-wave transient catalog. *Phys. Rev. D*, 103(12):122002, 2021.
- [59] R. Abbott et al. Tests of General Relativity with GWTC-3. 12 2021.
- [60] Kostas D. Kokkotas and Bernd G. Schmidt. Quasinormal modes of stars and black holes. *Living Rev. Rel.*, 2:2, 1999.
- [61] Emanuele Berti, Vitor Cardoso, and Andrei O. Starinets. Quasinormal modes of black holes and black branes. *Class. Quant. Grav.*, 26:163001, 2009.
- [62] R. A. Konoplya and A. Zhidenko. Quasinormal modes of black holes: From astrophysics to string theory. *Rev. Mod. Phys.*, 83:793–836, 2011.
- [63] Lionel London, Dairdre Shoemaker, and James Healy. Modeling ringdown: Beyond the fundamental quasinormal modes. *Phys. Rev. D*, 90(12):124032, 2014. [Erratum: Phys.Rev.D 94, 069902 (2016)].
- [64] Changfu Shi, Qingfei Zhang, and Jianwei Mei. Detectability and resolvability of quasinormal modes with space-based gravitational wave detectors. *Phys. Rev. D*, 110(12):124007, 2024.
- [65] Vladimir B. Braginsky and Kip S. Thorne. Gravitational-wave bursts with memory and experimental prospects. *Nature*, 327:123–125, 1987.
- [66] Shuo Sun, Changfu Shi, Jian-dong Zhang, and Jianwei Mei. Detecting the gravitational wave memory effect with TianQin. *Phys. Rev. D*, 107(4):044023, 2023.
- [67] Shuo Sun, Changfu Shi, Jian-dong Zhang, and Jianwei Mei. Bayesian analysis of the gravitational wave memory effect with TianQin. *Phys. Rev. D*, 110(2):024050, 2024.
- [68] G. W. Gibbons. Vacuum Polarization and the Spontaneous Loss of Charge by Black Holes.

- Commun. Math. Phys.*, 44:245–264, 1975.
- [69] Peter Goldreich and William H. Julian. Pulsar electrodynamics. *Astrophys. J.*, 157:869, 1969.
- [70] M. A. Ruderman and P. G. Sutherland. Theory of pulsars: Polar caps, sparks, and coherent microwave radiation. *Astrophys. J.*, 196:51, 1975.
- [71] R. D. Blandford and R. L. Znajek. Electromagnetic extractions of energy from Kerr black holes. *Mon. Not. Roy. Astron. Soc.*, 179:433–456, 1977.
- [72] Roy P. Kerr. Gravitational field of a spinning mass as an example of algebraically special metrics. *Phys. Rev. Lett.*, 11:237–238, 1963.
- [73] Olaf Dreyer, Bernard J. Kelly, Badri Krishnan, Lee Samuel Finn, David Garrison, and Ramon Lopez-Aleman. Black hole spectroscopy: Testing general relativity through gravitational wave observations. *Class. Quant. Grav.*, 21:787–804, 2004.
- [74] F. D. Ryan. Gravitational waves from the inspiral of a compact object into a massive, axisymmetric body with arbitrary multipole moments. *Phys. Rev. D*, 52:5707–5718, 1995.
- [75] Changfu Shi, Jiahui Bao, Haitian Wang, Jian-dong Zhang, Yiming Hu, Alberto Sesana, Enrico Barausse, Jianwei Mei, and Jun Luo. Science with the TianQin observatory: Preliminary results on testing the no-hair theorem with ringdown signals. *Phys. Rev. D*, 100(4):044036, 2019.
- [76] Tie-Guang Zi, Jian-Dong Zhang, Hui-Min Fan, Xue-Ting Zhang, Yi-Ming Hu, Changfu Shi, and Jianwei Mei. Science with the TianQin Observatory: Preliminary results on testing the no-hair theorem with extreme mass ratio inspirals. *Phys. Rev. D*, 104(6):064008, 2021.
- [77] Ying-Lin Kong and Jian-dong Zhang. Probing the spin-induced quadrupole moment of massive black holes with the inspiral of binary black holes. *Phys. Rev. D*, 110(2):024059, 2024.
- [78] D. M. Eardley, D. L. Lee, A. P. Lightman, R. V. Wagoner, and C. M. Will. Gravitational-wave observations as a tool for testing relativistic gravity. *Phys. Rev. Lett.*, 30:884–886, 1973.
- [79] D. M. Eardley, D. L. Lee, and A. P. Lightman. Gravitational-wave observations as a tool for testing relativistic gravity. *Phys. Rev. D*, 8:3308–3321, 1973.
- [80] B. P. Abbott et al. GW170814: A Three-Detector Observation of Gravitational Waves from a Binary Black Hole Coalescence. *Phys. Rev. Lett.*, 119(14):141101, 2017.
- [81] B. P. Abbott et al. Tests of General Relativity with GW170817. *Phys. Rev. Lett.*, 123(1):011102, 2019.
- [82] Peter T. H. Pang, Rico K. L. Lo, Isaac C. F. Wong, Tjonnjie G. F. Li, and Chris Van Den Broeck. Generic searches for alternative gravitational wave polarizations with networks of interferometric detectors. *Phys. Rev. D*, 101(10):104055, 2020.
- [83] Isaac C. F. Wong, Peter T. H. Pang, Rico K. L. Lo, Tjonnjie G. F. Li, and Chris Van Den Broeck. Null-stream-based Bayesian Unmodeled Framework to Probe Generic Gravitational-wave Polarizations. 5 2021.
- [84] Ning Xie, Jian-dong Zhang, Shun-Jia Huang, Yi-Ming Hu, and Jianwei Mei. Constraining the extra polarization modes of gravitational waves with double white dwarfs. *Phys. Rev. D*, 106(12):124017, 2022.
- [85] Mengke Ning, Jiangjin Zheng, and Jian-dong Zhang. In preparation.
- [86] Yu Hu, Pan-Pan Wang, Yu-Jie Tan, and Cheng-Gang Shao. Bayesian analysis of the stochastic gravitational-wave background with alternative polarizations for space-borne detectors. *Phys. Rev. D*, 107(2):024026, 2023.
- [87] Yu Hu, Pan-Pan Wang, Yu-Jie Tan, and Cheng-Gang Shao. Testing the Polarization of Gravitational-wave Background with the LISA-TianQin Network. *Astrophys. J.*, 961(1):116, 2024.
- [88] B. P. Abbott et al. GWTC-1: A Gravitational-Wave Transient Catalog of Compact Binary Mergers Observed by LIGO and Virgo during the First and Second Observing Runs. *Phys. Rev. X*, 9(3):031040, 2019.
- [89] R. Abbott et al. GWTC-2: Compact Binary Coalescences Observed by LIGO and Virgo During the First Half of the Third Observing Run. *Phys. Rev. X*, 11:021053, 2021.
- [90] R. Abbott et al. GWTC-3: Compact Binary Coalescences Observed by LIGO and Virgo during the Second Part of the Third Observing Run. *Phys. Rev. X*, 13(4):041039, 2023.
- [91] Emanuele Berti, Alessandra Buonanno, and Clifford M. Will. Estimating spinning binary parameters and testing alternative theories of gravity with LISA. *Phys. Rev. D*, 71:084025, 2005.
- [92] K. G. Arun, Bala R. Iyer, M. S. S. Qusailah, and B. S. Sathyaprakash. Testing post-Newtonian theory with gravitational wave observations. *Class. Quant. Grav.*, 23:L37–L43, 2006.
- [93] K. G. Arun, Bala R. Iyer, M. S. S. Qusailah, and B. S. Sathyaprakash. Probing the non-linear structure of general relativity with black hole binaries. *Phys. Rev. D*, 74:024006, 2006.
- [94] Nicolas Yunes and Frans Pretorius. Fundamental Theoretical Bias in Gravitational Wave

- Astrophysics and the Parameterized Post-Einsteinian Framework. *Phys. Rev. D*, 80:122003, 2009.
- [95] Sharaban Tahura and Kent Yagi. Parameterized Post-Einsteinian Gravitational Waveforms in Various Modified Theories of Gravity. *Phys. Rev. D*, 98(8):084042, 2018. [Erratum: *Phys.Rev.D* 101, 109902 (2020)].
- [96] Katie Chamberlain and Nicolas Yunes. Theoretical Physics Implications of Gravitational Wave Observation with Future Detectors. *Phys. Rev. D*, 96(8):084039, 2017.
- [97] Changfu Shi, Mujie Ji, Jian-dong Zhang, and Jianwei Mei. Testing general relativity with TianQin: The prospect of using the inspiral signals of black hole binaries. *Phys. Rev. D*, 108(2):024030, 2023.
- [98] Xulong Yuan, Jian-dong Zhang, and Jianwei Mei. Distinguish the environmental effects and modified theory of gravity with multiple massive black-hole binaries. 12 2024.
- [99] Ryuichi Takahashi and Takashi Nakamura. Wave effects in gravitational lensing of gravitational waves from chirping binaries. *Astrophys. J.*, 595:1039–1051, 2003.
- [100] Anna Liu, Rohit S. Chandramouli, Otto A. Hannuksela, Nicolás Yunes, and Tjonnje G. F. Li. Millilensing induced systematic biases in parameterized tests of General Relativity. 10 2024.
- [101] R. Abbott et al. Constraints on the Cosmic Expansion History from GWTC–3. *Astrophys. J.*, 949(2):76, 2023.
- [102] R. Abbott et al. Search for Gravitational-lensing Signatures in the Full Third Observing Run of the LIGO–Virgo Network. *Astrophys. J.*, 970(2):191, 2024.
- [103] Zucheng Gao, Xian Chen, Yi-Ming Hu, Jian-Dong Zhang, and Shun-Jia Huang. A higher probability of detecting lensed supermassive black hole binaries by LISA. *Mon. Not. Roy. Astron. Soc.*, 512(1):1–10, 2022.
- [104] Mesut Çalıřkan, Lingyuan Ji, Roberto Cotesta, Emanuele Berti, Marc Kamionkowski, and Sylvain Marsat. Observability of lensing of gravitational waves from massive black hole binaries with LISA. *Phys. Rev. D*, 107(4):043029, 2023.
- [105] Giovanni Tambalo, Miguel Zumalacárrregui, Liang Dai, and Mark Ho-Yeuk Cheung. Gravitational wave lensing as a probe of halo properties and dark matter. *Phys. Rev. D*, 108(10):103529, 2023.
- [106] Xin-yi Lin, Jian-dong Zhang, Liang Dai, Shun-Jia Huang, and Jianwei Mei. Detecting strong gravitational lensing of gravitational waves with TianQin. *Phys. Rev. D*, 108(6):064020, 2023.
- [107] T. J. M. Zouros and D. M. Eardley. INSTABILITIES OF MASSIVE SCALAR PERTURBATIONS OF A ROTATING BLACK HOLE. *Annals Phys.*, 118:139–155, 1979.
- [108] Steven L. Detweiler. KLEIN-GORDON EQUATION AND ROTATING BLACK HOLES. *Phys. Rev. D*, 22:2323–2326, 1980.
- [109] Sam R. Dolan. Instability of the massive Klein-Gordon field on the Kerr spacetime. *Phys. Rev. D*, 76:084001, 2007.
- [110] Asimina Arvanitaki, Masha Baryakhtar, and Xinlu Huang. Discovering the QCD Axion with Black Holes and Gravitational Waves. *Phys. Rev. D*, 91(8):084011, 2015.
- [111] Jun Zhang and Huan Yang. Dynamic Signatures of Black Hole Binaries with Superradiant Clouds. *Phys. Rev. D*, 101(4):043020, 2020.
- [112] Ning Xie and Fa Peng Huang. Imprints of ultralight axions on the gravitational wave and pulsar timing measurement. *Sci. China Phys. Mech. Astron.*, 67(1):210411, 2024.
- [113] Kazunari Eda, Yousuke Itoh, Sachiko Kuroyanagi, and Joseph Silk. New Probe of Dark-Matter Properties: Gravitational Waves from an Intermediate-Mass Black Hole Embedded in a Dark-Matter Minispikes. *Phys. Rev. Lett.*, 110(22):221101, 2013.
- [114] Kazunari Eda, Yousuke Itoh, Sachiko Kuroyanagi, and Joseph Silk. Gravitational waves as a probe of dark matter minispikes. *Phys. Rev. D*, 91(4):044045, 2015.
- [115] Asimina Arvanitaki and Sergei Dubovsky. Exploring the String Axiverse with Precision Black Hole Physics. *Phys. Rev. D*, 83:044026, 2011.
- [116] Asimina Arvanitaki, Masha Baryakhtar, Savas Dimopoulos, Sergei Dubovsky, and Robert Lasenby. Black Hole Mergers and the QCD Axion at Advanced LIGO. *Phys. Rev. D*, 95(4):043001, 2017.
- [117] Richard Brito, Shrobona Ghosh, Enrico Barausse, Emanuele Berti, Vitor Cardoso, Irina Dvorkin, Antoine Klein, and Paolo Pani. Stochastic and resolvable gravitational waves from ultralight bosons. *Phys. Rev. Lett.*, 119(13):131101, 2017.
- [118] Richard Brito, Shrobona Ghosh, Enrico Barausse, Emanuele Berti, Vitor Cardoso, Irina Dvorkin, Antoine Klein, and Paolo Pani. Gravitational wave searches for ultralight bosons with LIGO and LISA. *Phys. Rev. D*, 96(6):064050, 2017.
- [119] Masha Baryakhtar, Robert Lasenby, and Mae Teo. Black Hole Superradiance Signatures of

- Ultralight Vectors. *Phys. Rev. D*, 96(3):035019, 2017.
- [120] Nils Siemonsen and William E. East. Gravitational wave signatures of ultralight vector bosons from black hole superradiance. *Phys. Rev. D*, 101(2):024019, 2020.
- [121] Cristiano Palomba et al. Direct constraints on ultra-light boson mass from searches for continuous gravitational waves. *Phys. Rev. Lett.*, 123:171101, 2019.
- [122] R. Abbott et al. All-sky search for gravitational wave emission from scalar boson clouds around spinning black holes in LIGO O3 data. *Phys. Rev. D*, 105(10):102001, 2022.
- [123] Leo Tsukada, Richard Brito, William E. East, and Nils Siemonsen. Modeling and searching for a stochastic gravitational-wave background from ultralight vector bosons. *Phys. Rev. D*, 103(8):083005, 2021.
- [124] Jing Yang, Ning Xie, and Fa Peng Huang. Implication of nano-Hertz stochastic gravitational wave background on ultralight axion particles. *JCAP*, 11:045, 2024.
- [125] Xiao Wang, Fa Peng Huang, and Xinmin Zhang. Phase transition dynamics and gravitational wave spectra of strong first-order phase transition in supercooled universe. *JCAP*, 05:045, 2020.
- [126] Guy D. Moore and Tomislav Prokopec. How fast can the wall move? A Study of the electroweak phase transition dynamics. *Phys. Rev. D*, 52:7182–7204, 1995.
- [127] Xiao Wang, Fa Peng Huang, and Xinmin Zhang. Bubble wall velocity beyond leading-log approximation in electroweak phase transition. 11 2020.
- [128] Siyu Jiang, Fa Peng Huang, and Xiao Wang. Bubble wall velocity during electroweak phase transition in the inert doublet model. *Phys. Rev. D*, 107(9):095005, 2023.
- [129] Benoit Laurent and James M. Cline. First principles determination of bubble wall velocity. *Phys. Rev. D*, 106(2):023501, 2022.
- [130] Michael J. Baker, Joachim Kopp, and Andrew J. Long. Filtered Dark Matter at a First Order Phase Transition. *Phys. Rev. Lett.*, 125(15):151102, 2020.
- [131] Dongjin Chway, Tae Hyun Jung, and Chang Sub Shin. Dark matter filtering-out effect during a first-order phase transition. *Phys. Rev. D*, 101(9):095019, 2020.
- [132] Siyu Jiang, Fa Peng Huang, and Chong Sheng Li. Hydrodynamic effects on the filtered dark matter produced by a first-order phase transition. *Phys. Rev. D*, 108(6):063508, 2023.
- [133] E. Krylov, A. Levin, and V. Rubakov. Cosmological phase transition, baryon asymmetry and dark matter Q-balls. *Phys. Rev. D*, 87(8):083528, 2013.
- [134] Fa Peng Huang and Chong Sheng Li. Probing the baryogenesis and dark matter relaxed in phase transition by gravitational waves and colliders. *Phys. Rev. D*, 96(9):095028, 2017.
- [135] Jeong-Pyong Hong, Sunghoon Jung, and Ke-Pan Xie. Fermi-ball dark matter from a first-order phase transition. *Phys. Rev. D*, 102(7):075028, 2020.
- [136] Siyu Jiang, Aidi Yang, Jiucheng Ma, and Fa Peng Huang. Implication of nano-Hertz stochastic gravitational wave on dynamical dark matter through a dark first-order phase transition. *Class. Quant. Grav.*, 41(6):065009, 2024.
- [137] Siyu Jiang, Fa Peng Huang, and Pyungwon Ko. Gauged Q-ball dark matter through a cosmological first-order phase transition. *JHEP*, 07:053, 2024.
- [138] Xin-min Zhang. Operators analysis for Higgs potential and cosmological bound on Higgs mass. *Phys. Rev. D*, 47:3065–3067, 1993.
- [139] Christophe Grojean, Geraldine Servant, and James D. Wells. First-order electroweak phase transition in the standard model with a low cutoff. *Phys. Rev. D*, 71:036001, 2005.
- [140] Fa Peng Huang, Pei-Hong Gu, Peng-Fei Yin, Zhao-Huan Yu, and Xinmin Zhang. Testing the electroweak phase transition and electroweak baryogenesis at the LHC and a circular electron-positron collider. *Phys. Rev. D*, 93(10):103515, 2016.
- [141] Fa Peng Huang, Youping Wan, Dong-Gang Wang, Yi-Fu Cai, and Xinmin Zhang. Hearing the echoes of electroweak baryogenesis with gravitational wave detectors. *Phys. Rev. D*, 94(4):041702, 2016.
- [142] Rong-Gen Cai, Misao Sasaki, and Shao-Jiang Wang. The gravitational waves from the first-order phase transition with a dimension-six operator. *JCAP*, 08:004, 2017.
- [143] N. Aghanim et al. Planck 2018 results. VI. Cosmological parameters. *Astron. Astrophys.*, 641:A6, 2020. [Erratum: *Astron. Astrophys.* 652, C4 (2021)].
- [144] Adam G. Riess et al. A Comprehensive Measurement of the Local Value of the Hubble Constant with $1 \text{ km s}^{-1} \text{ Mpc}^{-1}$ Uncertainty from the Hubble Space Telescope and the SH0ES Team. *Astrophys. J. Lett.*, 934(1):L7, 2022.
- [145] Adam G. Riess et al. JWST Validates HST Distance Measurements: Selection of Supernova Subsample Explains Differences in JWST Estimates of Local H_0 . *Astrophys. J.*, 977(1):120, 2024.
- [146] Wendy L. Freedman. Cosmology at a Crossroads. *Nature Astron.*, 1:0121, 2017.

- [147] Adam G. Riess. The Expansion of the Universe is Faster than Expected. *Nature Rev. Phys.*, 2(1):10–12, 2019.
- [148] Leandros Perivolaropoulos and Foteini Skara. Challenges for Λ CDM: An update. *New Astron. Rev.*, 95:101659, 2022.
- [149] Eleonora Di Valentino, Olga Mena, Supriya Pan, Luca Visinelli, Weiqiang Yang, Alessandro Melchiorri, David F. Mota, Adam G. Riess, and Joseph Silk. In the realm of the Hubble tension—a review of solutions. *Class. Quant. Grav.*, 38(15):153001, 2021.
- [150] Nils Schöneberg, Guillermo Franco Abellán, Andrea Pérez Sánchez, Samuel J. Witte, Vivian Poulin, and Julien Lesgourgues. The H0 Olympics: A fair ranking of proposed models. *Phys. Rept.*, 984:1–55, 2022.
- [151] Rong-Gen Cai, Zong-Kuan Guo, Shao-Jiang Wang, Wang-Wei Yu, and Yong Zhou. No-go guide for the Hubble tension: Late-time solutions. *Phys. Rev. D*, 105(2):L021301, 2022.
- [152] Gong-Bo Zhao et al. Dynamical dark energy in light of the latest observations. *Nature Astron.*, 1(9):627–632, 2017.
- [153] Zhenyu Zhang, Gan Gu, Xiaoma Wang, Yun-He Li, Cristiano G. Sabiu, Hyunbae Park, Haitao Miao, Xiaolin Luo, Feng Fang, and Xiao-Dong Li. Non-parametric dark energy reconstruction using the tomographic Alcock-Paczynski test. *Astrophys. J.*, 878(2):137, 2019.
- [154] A. G. Adame et al. DESI 2024 VI: Cosmological Constraints from the Measurements of Baryon Acoustic Oscillations. 4 2024.
- [155] Bernard F. Schutz. Determining the Hubble Constant from Gravitational Wave Observations. *Nature*, 323:310–311, 1986.
- [156] Dragoljub Markovic. On the possibility of determining cosmological parameters from measurements of gravitational waves emitted by coalescing, compact binaries. *Phys. Rev. D*, 48:4738–4756, 1993.
- [157] Daniel E. Holz and Scott A. Hughes. Using gravitational-wave standard sirens. *Astrophys. J.*, 629:15–22, 2005.
- [158] B. P. Abbott et al. A gravitational-wave standard siren measurement of the Hubble constant. *Nature*, 551(7678):85–88, 2017.
- [159] M. Soares-Santos et al. First Measurement of the Hubble Constant from a Dark Standard Siren using the Dark Energy Survey Galaxies and the LIGO/Virgo Binary–Black-hole Merger GW170814. *Astrophys. J. Lett.*, 876(1):L7, 2019.
- [160] B. P. Abbott et al. A Gravitational-wave Measurement of the Hubble Constant Following the Second Observing Run of Advanced LIGO and Virgo. *Astrophys. J.*, 909(2):218, 2021.
- [161] Pau Amaro Seoane et al. Astrophysics with the Laser Interferometer Space Antenna. *Living Rev. Rel.*, 26(1):2, 2023.
- [162] Pierre Auclair et al. Cosmology with the Laser Interferometer Space Antenna. *Living Rev. Rel.*, 26(1):5, 2023.
- [163] Walter Del Pozzo, Alberto Sesana, and Antoine Klein. Stellar binary black holes in the LISA band: a new class of standard sirens. *Mon. Not. Roy. Astron. Soc.*, 475(3):3485–3492, 2018.
- [164] Niccolò Muttoni, Alberto Mangiagli, Alberto Sesana, Danny Laghi, Walter Del Pozzo, David Izquierdo-Villalba, and Mattia Rosati. Multiband gravitational wave cosmology with stellar origin black hole binaries. *Phys. Rev. D*, 105(4):043509, 2022.
- [165] Liang-Gui Zhu, Ling-Hua Xie, Yi-Ming Hu, Shuai Liu, En-Kun Li, Nicola R. Napolitano, Bai-Tian Tang, Jian-dong Zhang, and Jianwei Mei. Constraining the Hubble constant to a precision of about 1% using multi-band dark standard siren detections. *Sci. China Phys. Mech. Astron.*, 65(5):259811, 2022.
- [166] Chelsea L. MacLeod and Craig J. Hogan. Precision of Hubble constant derived using black hole binary absolute distances and statistical redshift information. *Phys. Rev. D*, 77:043512, 2008.
- [167] Danny Laghi, Nicola Tamanini, Walter Del Pozzo, Alberto Sesana, Jonathan Gair, Stanislav Babak, and David Izquierdo-Villalba. Gravitational-wave cosmology with extreme mass-ratio inspirals. *Mon. Not. Roy. Astron. Soc.*, 508(3):4512–4531, 2021.
- [168] Liang-Gui Zhu, Hui-Min Fan, Xian Chen, Yi-Ming Hu, and Jian-dong Zhang. Improving Cosmological Constraints by Inferring the Formation Channel of Extreme-mass-ratio Inspirals. *Astrophys. J. Suppl.*, 273(2):24, 2024.
- [169] Antoine Petiteau, Stanislav Babak, and Alberto Sesana. Constraining the dark energy equation of state using LISA observations of spinning Massive Black Hole binaries. *Astrophys. J.*, 732:82, 2011.
- [170] Nicola Tamanini, Chiara Caprini, Enrico Barausse, Alberto Sesana, Antoine Klein, and Antoine Petiteau. Science with the space-based interferometer eLISA. III: Probing the expansion of

- the Universe using gravitational wave standard sirens. *JCAP*, 04:002, 2016.
- [171] Liang-Gui Zhu, Yi-Ming Hu, Hai-Tian Wang, Jian-dong Zhang, Xiao-Dong Li, Martin Hendry, and Jianwei Mei. Constraining the cosmological parameters using gravitational wave observations of massive black hole binaries and statistical redshift information. *Phys. Rev. Res.*, 4(1):013247, 2022.
- [172] Kevin J. Shuman and Neil J. Cornish. Massive black hole binaries and where to find them with dual detector networks. *Phys. Rev. D*, 105(6):064055, 2022.
- [173] Jie Gao, Yi-Ming Hu, En-Kun Li, Jian-dong Zhang, and Jianwei Mei. Bayesian parameter estimation of massive black hole binaries with TianQin and LISA. *Phys. Rev. D*, 111(2):023039, 2025.
- [174] Xiangyu Lyu, En-Kun Li, and Yi-Ming Hu. Parameter estimation of stellar mass binary black holes in the network of TianQin and LISA. *Phys. Rev. D*, 108(8):083023, 2023.
- [175] Tamara Bogdanovic, M. Coleman Miller, and Laura Blecha. Electromagnetic counterparts to massive black-hole mergers. *Living Rev. Rel.*, 25(1):3, 2022.
- [176] M. Punturo et al. The Einstein Telescope: A third-generation gravitational wave observatory. *Class. Quant. Grav.*, 27:194002, 2010.
- [177] Benjamin P Abbott et al. Exploring the Sensitivity of Next Generation Gravitational Wave Detectors. *Class. Quant. Grav.*, 34(4):044001, 2017.
- [178] Stanislav Babak, Jonathan Gair, Alberto Sesana, Enrico Barausse, Carlos F. Sopuerta, Christopher P. L. Berry, Emanuele Berti, Pau Amaro-Seoane, Antoine Petiteau, and Antoine Klein. Science with the space-based interferometer LISA. V: Extreme mass-ratio inspirals. *Phys. Rev. D*, 95(10):103012, 2017.
- [179] Pau Amaro-Seoane. Relativistic dynamics and extreme mass ratio inspirals. *Living Rev. Rel.*, 21(1):4, 2018.
- [180] Yuri Levin. Starbursts near supermassive black holes: young stars in the Galactic Center, and gravitational waves in LISA band. *Mon. Not. Roy. Astron. Soc.*, 374:515–524, 2007.
- [181] Zhen Pan and Huan Yang. Formation Rate of Extreme Mass Ratio Inspirals in Active Galactic Nuclei. *Phys. Rev. D*, 103(10):103018, 2021.
- [182] Zhen Pan, Zhenwei Lyu, and Huan Yang. Wet extreme mass ratio inspirals may be more common for spaceborne gravitational wave detection. *Phys. Rev. D*, 104(6):063007, 2021.
- [183] Ling-Feng Wang, Ze-Wei Zhao, Jing-Fei Zhang, and Xin Zhang. A preliminary forecast for cosmological parameter estimation with gravitational-wave standard sirens from TianQin. *JCAP*, 11:012, 2020.
- [184] Antoine Klein et al. Science with the space-based interferometer eLISA: Supermassive black hole binaries. *Phys. Rev. D*, 93(2):024003, 2016.
- [185] Shun-Jia Huang, Yi-Ming Hu, Xian Chen, Jian-dong Zhang, En-Kun Li, Zucheng Gao, and Xin-Yi Lin. Measuring the Hubble constant using strongly lensed gravitational wave signals. *JCAP*, 08:003, 2023.
- [186] Michel Chevallier and David Polarski. Accelerating universes with scaling dark matter. *Int. J. Mod. Phys. D*, 10:213–224, 2001.
- [187] Eric V. Linder. Exploring the expansion history of the universe. *Phys. Rev. Lett.*, 90:091301, 2003.
- [188] P. J. E. Peebles and Bharat Ratra. The Cosmological Constant and Dark Energy. *Rev. Mod. Phys.*, 75:559–606, 2003.
- [189] Sean M. Carroll. The Cosmological constant. *Living Rev. Rel.*, 4:1, 2001.
- [190] Miao Li, Xiao-Dong Li, Shuang Wang, and Yi Wang. Dark Energy. *Commun. Theor. Phys.*, 56:525–604, 2011.
- [191] NASA Gravitational-wave mission concept study final report, 2012.
- [192] Bo-Bing Ye, Xuefeng Zhang, Ming-Yue Zhou, Yan Wang, Hui-Min Yuan, Defeng Gu, Yanwei Ding, Jinxiu Zhang, Jianwei Mei, and Jun Luo. Optimizing orbits for TianQin. *Int. J. Mod. Phys. D*, 28(09):09, 2019.
- [193] Bobing Ye and Xuefeng Zhang. Effects of lunisolar perturbations on TianQin constellation: An analytical model. *Phys. Rev. D*, 109(8):083033, 2024.
- [194] Ming-Yue Zhou, Xin-Chun Hu, Bobing Ye, Shoucun Hu, Dong-Dong Zhu, Xuefeng Zhang, Wei Su, and Yan Wang. Orbital effects on time delay interferometry for TianQin. *Phys. Rev. D*, 103(10):103026, 2021.
- [195] Zhuangbin Tan, Bobing Ye, and Xuefeng Zhang. Impact of orbital orientations and radii on TianQin constellation stability. *Int. J. Mod. Phys. D*, 29(08):08, 2020.
- [196] Xuefeng Zhang, Chengjian Luo, Lei Jiao, Bobing Ye, Huimin Yuan, Lin Cai, Defeng Gu, Jianwei Mei, and Jun Luo. Effect of Earth-Moon’s gravity on TianQin’s range acceleration noise. *Phys. Rev. D*, 103(6):062001, 2021.

- [197] Chengjian Luo and Xuefeng Zhang. Effect of Earth-Moon's gravity on TianQin's range acceleration noise. II. Impact of orbit selection. *Phys. Rev. D*, 105(10):102007, 2022.
- [198] Lei Jiao and Xuefeng Zhang. Effect of Earth-Moon's gravity on TianQin's range acceleration noise. III. An analytical model. *Phys. Rev. D*, 107(10):102004, 2023.
- [199] Kun Liu, Chengjian Luo, and Xuefeng Zhang. Effect of solar free oscillations on TianQin's range acceleration noise. *Class. Quant. Grav.*, 40(19):197001, 2023.
- [200] Lu Zheng, Shutao Yang, and Xuefeng Zhang. Doppler effect in TianQin time-delay interferometry. *Phys. Rev. D*, 108(2):022001, 2023.
- [201] Xuefeng Zhang, Hongyin Li, and Jianwei Mei. Thermal stability estimation of TianQin satellites based on LISA-like thermal design concept. internal technical report (in Chinese), May 2018.
- [202] Houyuan Chen, Chen Ling, Xuefeng Zhang, Xin Zhao, Ming Li, and Yanwei Ding. Thermal environment analysis for TianQin. *Class. Quant. Grav.*, 38(15):155015, 2021.
- [203] Dong Wang, Xuefeng Zhang, Lihua Zhang, and Ming Li. Long-term thermal stability of TianQin satellites. *Phys. Rev. D*, 109(10):102007, 2024.
- [204] Ling-Feng Lu, Wei Su, Xuefeng Zhang, Zhao-Guo He, Hui-Zong Duan, Yuan-Ze Jiang, and Hsien-Chi Yeh. Effects of the Space Plasma Density Oscillation on the Interspacecraft Laser Ranging for TianQin Gravitational Wave Observatory. *J. Geophys. Res. Space Phys.*, 126(2):e2020JA028579, 2021.
- [205] Wei Su et al. Analyses of Laser Propagation Noises for TianQin Gravitational Wave Observatory Based on the Global Magnetosphere MHD Simulations. *Astrophys. J.*, 914(2):139, 2021.
- [206] Yi-De Jing, Lu Zheng, Shutao Yang, Xuefeng Zhang, Lingfeng Lu, Binbin Tang, and Wei Su. Plasma noise in TianQin time-delay interferometry. *Phys. Rev. D*, 106(8):082006, 2022.
- [207] Liu YaNan, Su Wei, Zhang XueFeng, Zhang JiXiang, and Zhou ShenWei. Solar Plasma Noise in TianQin Laser Propagation: An Extreme Case and Statistical Analysis. *Astrophys. J.*, 975(2):291, 2024.
- [208] Xuefeng Zhang and TianQin Team. How to detect gravitational waves in high Earth orbits? –TianQin mission design overview. Presentation at the 7th International Workshop on the TianQin Science Mission, April 2024.
- [209] Bobing Ye, Xuefeng Zhang, Yanwei Ding, and Yunhe Meng. Eclipse avoidance in TianQin orbit selection. *Phys. Rev. D*, 103(4):042007, 2021.
- [210] Xuefeng Zhang, Bobing Ye, Zhuangbin Tan, Huimin Yuan, Chengjian Luo, Lei Jiao, Defeng Gu, Yanwei Ding, and Jianwei Mei. Orbit and constellation design for TianQin: progress review (in chinese). *Acta Scientiarum Naturalium Universitatis Sunyatseni*, 60(1-2):123–128, 2021.
- [211] Gábor Tóth, Igor V Sokolov, Tamas I Gombosi, David R Chesney, C Robert Clauer, Darren L De Zeeuw, Kenneth C Hansen, Kevin J Kane, Ward B Manchester, Robert C Oehmke, et al. Space weather modeling framework: A new tool for the space science community. *Journal of Geophysical Research: Space Physics*, 110(A12), 2005.
- [212] Yuzhou Fang, Xuefeng Zhang, Fangyuan Fu, and Hongyin Li. Payload architecture and pointing control strategies for TianQin. *Phys. Rev. D*, 109(6):062001, 2024.
- [213] Dezhi Wang, Xuefeng Zhang, and Hui-Zong Duan. On point-ahead angle control strategies for TianQin. *Class. Quant. Grav.*, 41(11):117003, 2024.
- [214] Zhizhao Wang, Shuju Yang, Kaihang Wu, Xiaojie Wang, Huizong Duan, Xuefeng Zhang, Hsien-Chi Yeh, and Yurong Liang. Postprocessing of tilt-to-length noise with coefficient drifts in TianQin using a null time-delay interferometry channel. *Phys. Rev. D*, 111(4):042004, 2025.
- [215] Dexuan Zhang, Xiaorong Ye, Hongyin Li, Guoying Zhao, and Junxiang Lian. Nonlinear modeling and validation of spacecraft dynamics for space-based gravitational wave detector. *Acta Astronautica*, 224:57–68, 2024.
- [216] Lihua Zhang, Ming Li, Yongxin Gao, Yuexin Hu, Fengbin Wang, and Tao Zhang. The spacecraft system and platform technologies for gravitational wave detection in space (in chinese). *Acta Scientiarum Naturalium Universitatis Sunyatseni*, 60(Z1):129–137, 2021.
- [217] Xuefeng Zhang, Dong Wang, and Hongyin Li. A satellite platform configuration for geocentric high-orbit space gravitational wave detection, May 2023.
- [218] Zhenghao Zhang, Yong Huang, Peng Yang, Yanling Chen, and Xiaolin Jia. Orbit determination analysis of igso satellite onboard gps/bds pseudorange data corrected by different code hardware delays products. *Advances in Space Research*, 75(3):3050–3062, 2025.
- [219] Lisheng Tong, Kai Shao, Defeng Gu, Chengjun Yang, Chunbo Wei, Zicong An, Zheyu Xu, Jubo Zhu, Jian Wang, and Daoping Liu. Accuracy analysis of orbit determination for high earth orbit gravitational wave detectors using multi-gnss sidelobe signals. *Acta Astronautica*, 229:534–546, 2025.

- [220] Zicong An, Kai Shao, Defeng Gu, Jubo Zhu, Ming Li, Lisheng Tong, and Chunbo Wei. Simulation and accuracy analysis of orbit determination for TianQin using SLR data. *Class. Quant. Grav.*, 39(24):245016, 2022.
- [221] Caishi Zhang et al. The facilities and performance of TianQin laser ranging station. *Class. Quant. Grav.*, 39(12):125005, 2022.
- [222] Zicong An, Kai Shao, Defeng Gu, Chunbo Wei, Lisheng Tong, Zheyu Xu, Ming Li, and Jian Wang. Analysis and comparison of the orbit determination accuracy of TianQin based on multiple ground-based measurements. *Phys. Scripta*, 99(8):085003, 2024.
- [223] Zhaoxiang Yi, Lin Sun, and Meng Jiang. Data transmission analysis and communication scheme design for tianqin mission. *IEEE Access*, 12:42585–42593, 2024.
- [224] Jia Hao, Fulong Wei, Xingyu Yan, Jinlong Ma, Zebing Zhou, and Xiaobing Luo. The influence of temperature disturbance on space inertial sensors. *Sensors*, 24(21):6934, 2024.
- [225] Siqi Zhang, Jiale Peng, Chao Deng, Fulong Wei, Jiacheng Li, Jinlong Ma, and Xiaobing Luo. An integrated downhole thermal management system with improved operating thermal performance and rapid post-operation air cooling. *Applied Thermal Engineering*, 257:124473, 2024.
- [226] Zeyu Wang, Run Hu, Xiaobing Luo, and Jinlong Ma. Compositionally restricted atomistic line graph neural network for improved thermoelectric transport property predictions. *Journal of Applied Physics*, 136(15):155103, 10 2024.
- [227] Guoqing Sun, Zheng Xiang, Jinlong Ma, Xiaobing Luo, and Dongwei Xu. Thermal conductivity at finite temperature and electronic structure of the ultra-wide band gap fluorinated 2d gan. *Journal of Physics: Condensed Matter*, 36(1):015301, sep 2023.
- [228] Huaiyu Zuo, Song Xue, Tao Hong, Guanying Xing, Jiacheng Han, Jinlong Ma, Run Hu, and Xiaobing Luo. Theoretical and experimental analysis of the centrifugal micro hydrodynamic axial-thrust bearing. *Tribology International*, 187:108696, 2023.
- [229] Guoqing Sun, Jinlong Ma, Chenhan Liu, Zheng Xiang, Dongwei Xu, Te-Huan Liu, and Xiaobing Luo. Four-phonon and normal scattering in 2d hexagonal structures. *International Journal of Heat and Mass Transfer*, 215:124475, 2023.
- [230] Guoqing Sun, Zheng Xiang, Jinlong Ma, Xiaobing Luo, and Dongwei Xu. Opposite atom dependence of isotope engineering of thermal conductivity in bulk and 2d gan. *Nanotechnology*, 34(48):485404, sep 2023.
- [231] Xuanyao Bai, Kailun Wen, Donghong Peng, Shuangqiang Liu, and Le Luo. Atomic magnetometers and their application in industry. *Frontiers in Physics*, 11:1212368, June 2023.
- [232] Chaoqun Ma, Donghong Peng, Xuanyao Bai, Shuangqiang Liu, and Le Luo. A review of optical fiber sensing technology based on thin film and fabry–perot cavity. *Coatings*, 2023.
- [233] Wenwen Qu, Yanxia Chen, Chaoqun Ma, Donghong Peng, Xuanyao Bai, Jiaxin Zhao, Shuangqiang Liu, and Le Luo. Application of optical fiber sensing technology and coating technology in blood component detection and monitoring. *Coatings (2079-6412)*, 14(2), 2024.
- [234] Kailun Wen, Xuanyao Bai, Shuangqiang Liu, and Le Luo. Research on Solid-state Optical Filtering Technology Using Faraday Anomalous Dispersion in Rare Earth-doped Crystals. In *Journal of Physics Conference Series*, volume 2617 of *Journal of Physics Conference Series*, page 012001. IOP, October 2023.
- [235] Xuanyao Bai, Donghong Peng, Yanxia Chen, Chaoqun Ma, Wenwen Qu, Shuangqiang Liu, and Le Luo. Three-dimensional electrochemical-magnetic-thermal coupling model for lithium-ion batteries and its application in battery health monitoring and fault diagnosis. *Scientific Reports*, 14:10802, May 2024.
- [236] Donghong Peng, Chaoqun Ma, Xuanyao Bai, Yanxia Chen, Wenwen Qu, Shuangqiang Liu, and Le Luo. An improved two-point localization method with reduced blind spots based on magnetic gradient tensor. *Measurement*, 240:115538, January 2025.
- [237] Chaoqun Ma, Yanxia Chen, Wenwen Qu, Donghong Peng, Xuanyao Bai, Shuangqiang Liu, and Le Luo. High-sensitivity fiber temperature and pressure sensor based on fabry-perot interferometry and Vernier effect. *Optics Laser Technology*, 181:111999, February 2025.
- [238] Yelong Tong, Xin Zhao, Hong Jin, Xisheng Shao, Lei Liu, Shitao Ren, and Ran Wei. Research on high stability thermal control system based on reconfigurable distributed temperature control. *Advanced Small Satellite Technology (in Chinese and English)*, 1(1):113–121, 2024.
- [239] Yin-Fa Yang, Jian-Min Hao, Wei Zhang, Yi-Tao Shen, Rui Zhou, Hua Chen, and Wen-Long Cheng. High-precision adaptive temperature control performance of thin positive temperature coefficient materials with ultra-high resistance-temperature coefficient. *Applied Thermal Engineering*, 253:123767, 2024.

- [240] Li-Kai Mao, Qun Liu, Hua Chen, and Wen-Long Cheng. A novel model of the anisotropic thermal conductivity of composite phase change materials under compression. *International Journal of Heat and Mass Transfer*, 227:125512, 2024.
- [241] Qi Deng, Hua Chen, Changpeng Yang, Xin Zhao, and Wen long Cheng. Study on transient heat transfer characteristics of heat flow under low frequency periodic thermal boundary conditions. *International Communications in Heat and Mass Transfer*, 159:108021, 2024.
- [242] Jian-Min Hao, Yin-Fa Yang, Yi-Tao Shen, Rui Zhou, Wei Zhang, Hua Chen, and Wen-Long Cheng. Positive temperature coefficient material based on silicone rubber/paraffin/ graphite/ carbon nanotubes for wearable thermal management devices. *Chemical Engineering Journal*, 493:152427, 2024.
- [243] Hua Chen, Jia-He Kang, Rui Zhao, Chang-Peng Yang, Xin Zhao, and Wen-Long Cheng. Study on temperature noise suppression characteristics of passive thermal control materials in gravitational wave detection. *Class. Quant. Grav.*, 41(19):195025, 2024.
- [244] Sizhao Zhang, Chun Liu, Zhao Wang, Jing Wang, Guangyu Xu, and Hongwei Shi. Ultralow shrinkage polyimide hybrid aerogel composite enhanced with organic fibers for thermal protection. *Journal of Applied Polymer Science*, 141(31/32):n/a, 1 2024.
- [245] Sizhao Zhang, Chun Liu, Yonggang Jiang, and Jian Feng. Research progress on high temperature resistance of polyimide aerogels. *Material Introduction*, 38(13):280–290, 7 2024.
- [246] Shaoying Kang, Ran Wei, Ming Li, Xin Zhang, Xin Zhao, Qiang Xin, and Yuexin Hu. A method for identifying static characteristics of high precision temperature measurement on orbit. In Yue Wang, Jiaqi Zou, Lexi Xu, Zhilei Ling, and Xinzhou Cheng, editors, *Signal and Information Processing, Networking and Computers*, pages 61–65, Singapore, 2024. Springer Nature Singapore.
- [247] Ao Lou, Yuan Yang Yu, Bu Tian Zhang, Yi Liu, Quan Fu, Jian Kang Zhang, Hua Hua Fu, Shun Wang, and Ze Bing Zhou. Theoretical Calculations and Experimental Measurements on the Two-Component $\mathrm{Au}\text{-Pt}$ Alloys with Ultralow Magnetic Susceptibility. *Physical Review Applied*, 19(3):034080, March 2023.
- [248] Xiao Tian Yang, Ming Hu, Cheng Rui Wang, Duo Li, De Cong Chen, Chao Li Ou Yang, Yan Zheng Bai, Shao Bo Qu, and Ze Bing Zhou. A method for high-precision measuring differential transformer asymmetry. *Review of Scientific Instruments*, 94(6):065006, June 2023.
- [249] Hong Gang Li, Gui Lin Li, Wei Hong, Bing Xue Chen, Liang Yu Chu, Meng Hao Zhao, Chun Yu Xiao, Bo Wen Jia, Yan Zheng Bai, and Ze Bing Zhou. Capacitive Sensing-Based Charge Measurement for Space Inertial Sensors. *IEEE Transactions on Instrumentation and Measurement*, 73:1–9, 2024.
- [250] Ming Hu, Yan Zheng Bai, Ze Bing Zhou, Zhu Xi Li, and Jun Luo. Resonant frequency detection and adjustment method for a capacitive transducer with differential transformer bridge. *Review of Scientific Instruments*, 85(5):055001, May 2014.
- [251] Y. Z. Bai, L. Fang, J. Luo, H. Yin, and Z. B. Zhou. Improving the measurement sensitivity of angular deflection of a torsion pendulum by an electrostatic spring. *Class. Quant. Grav.*, 32(17):175018, 2015.
- [252] Yan Zheng Bai, Ze Bing Zhou, Hai Bo Tu, Shu Chao Wu, Lin Cai, Li Liu, and Jun Luo. Capacitive position measurement for high-precision space inertial sensor. *Frontiers of Physics in China*, 4(2):205–208, June 2009.
- [253] Fang Chao Yang, Yan Zheng Bai, Wei Hong, Honggang Li, Li Liu, Timothy J. Sumner, Quan Feng Yang, Yu Jie Zhao, and Zebing Zhou. Investigation of charge management using UV LED device with a torsion pendulum for TianQin. *Classical and Quantum Gravity*, 37(11):115005, May 2020.
- [254] Fang Chao Yang, Yan Zheng Bai, Wei Hong, Timothy J. Sumner, and Ze Bing Zhou. A charge control method for space-mission inertial sensor using differential UV LED emission. *Review of Scientific Instruments*, 91(12):124502, December 2020.
- [255] Hong Gang Li, Quan Feng Yang, Fang Chao Yang, Wei Hong, Yan Zheng Bai, and Ze Bing Zhou. Coupling efficiency improvement of light source with a convex lens for space charge managements. *Optik*, 248:167999, December 2021.
- [256] Bing Xue Chen, Wei Hong, Hong Gang Li, Meng Hao Zhao, Liang Yu Chu, Qing Qing Li, Bo Wen Jia, Deng Zhang, Yan Zheng Bai, and Ze Bing Zhou. Using finite element simulation to evaluate charge measurement precision for space inertial sensors. *Measurement Science and Technology*, 35(4):045026, January 2024.
- [257] Chao Xue et al. Progress and prospects of test mass locking and release technology in space inertial sensor. *China Basic Science*, 26(5):1–11,27, 10 2024.
- [258] Di-Wen Shi, Ji Wang, Chao Xue, Biao Yang, Jie Chang, Bing-Wei Cai, Yi-Yan Xu, Wei Wang,

- and Shan-Qing Yang. Development of a dynamical model and control methodology for the actuator of the grabbing positioning and release mechanism in tianqin. *Advances in Space Research*, 2025.
- [259] Hang Yin, Yan-Zheng Bai, Ming Hu, Li Liu, Jun Luo, Ding-Yin Tan, Hsien-Chi Yeh, and Ze-Bing Zhou. Measurements of temporal and spatial variation of surface potential using a torsion pendulum and a scanning conducting probe. *Phys. Rev. D*, 90(12):122001, 2014.
- [260] Hang Yin, Ding Yin Tan, Ming Hu, Shun Wang, Yan Zheng Bai, Shu Chao Wu, and Ze Bing Zhou. Measurements of Magnetic Properties of Kilogram-Level Test Masses for Gravitational-Wave Detection Using a Torsion Pendulum. *Physical Review Applied*, 15(1):014008, January 2021.
- [261] Chi Song, Ming Hu, Ke Li, Peng Shun Luo, Shun Wang, Hang Yin, and Ze Bing Zhou. A high precision surface potential imaging torsion pendulum facility to investigate physical mechanism of patch effect. *Review of Scientific Instruments*, 94(2):024501, February 2023.
- [262] Guilin Li et al. Thermal induced noise on test mass with copper alloy electrode housing for spaceborne gravitational wave detection. *Phys. Rev. D*, 109(8):082001, 2024.
- [263] Yu Jie Zhao, Gui Lin Li, Li Liu, Cheng Gang Shao, Ding Yin Tan, Hang Yin, and Ze Bing Zhou. Experimental Verification of and Physical Interpretation for Adsorption-Dependent Squeeze-Film Damping. *Physical Review Applied*, 19(4):044005, April 2023.
- [264] Shufan Wu, Luisella Giulicchi, Thomas Fenal, and Mark Watt. Attitude stabilization of lisa pathfinder spacecraft using colloidal micro-newton thrusters. In *AIAA Guidance, Navigation, and Control Conference*, page 8198, 2010.
- [265] Fulvio Ricci. Gravitational Waves Detectors. *J. Phys. Conf. Ser.*, 1468(1):012224, 2020.
- [266] G Noci, Giovanni Matticari, P Siciliano, L Fallerini, L Boschini, and V Vettorello. Cold gas micro propulsion system for scientific satellite fine pointing: Review of development and qualification activities at thales alenia space italia. In *45th AIAA/ASME/SAE/ASEE Joint Propulsion Conference & Exhibit*, page 5127, 2009.
- [267] M. Armano et al. LISA Pathfinder micronewton cold gas thrusters: In-flight characterization. *Phys. Rev. D*, 99(12):122003, 2019.
- [268] AM Mel'nik and AK Dambis. Kinematics of ob associations and the first data from the gaia satellite. *Astronomy Reports*, 62:998–1002, 2018.
- [269] Hao-Yuan Zhang, Jian-Ping Liu, Shao-Gang Hu, Jin-Huan Yin, Yuan Zhong, Zhu Li, and Shan-Qing Yang. A high resolution and wide range valve for micronewton cold gas thrusters. *Review of Scientific Instruments*, 95(2), 2024.
- [270] F. P. An et al. The Detector System of The Daya Bay Reactor Neutrino Experiment. *Nucl. Instrum. Meth. A*, 811:133–161, 2016.
- [271] Jun Luo et al. The first round result from the TianQin-1 satellite. *Class. Quant. Grav.*, 37(18):185013, 2020.
- [272] Xingyu Gou, Lijiao Wang, Mingqun Li, Qinhua Jiang, and Shaokai Wang. Acceleration mode drag-free control of tq-1 satellite. *Journal of Astronautics (in Chinese)*, 42(5):603–610, 2021.
- [273] Xingyu Gou, Lijiao Wang, Xianmin Xu, Kui Zou, and Qinhua Jiang. Study on dynamic coordination condition of displacement drag-free control. *Journal of Astronautics (in Chinese)*, 45(4):539–548, 2024.
- [274] Kui Zou and Xingyu Gou. Characteristic model-based all-coefficient adaptive control of the drag-free satellites. In *2020 Chinese Automation Congress (CAC)*, pages 2839–2844, 2020.
- [275] Lijiao Wang, Xingyu Gou, Qirui Liu, and Bin Meng. Adaptive drag-free control of gravity field satellites via a modified characteristic model-based approach. *Lecture Notes in Electrical Engineering*, 644:529–538, October 2021.
- [276] Shuping Tan, Jin Guo, Yanlong Zhao, and Jifeng Zhang. Adaptive control with saturation-constrained observations for drag-free satellites—a set-valued identification approach. *SCIENCE CHINA*, 64(010):202202, October 2021.
- [277] Fei Yang, Shuping Tan, Wenchao Xue, Jin Guo, and Yanlong Zhao. Extended state filtering with saturation-constrained observations and active disturbance rejection control of position and attitude for drag-free satellites. *Acta Automatica Sinica (in Chinese)*, 46(11):2337–2349, 2020.
- [278] Xiaobin Lian, Jinxiu Zhang, Lang Lu, Jihe Wang, Lixuan Liu, Jun Sun, and Yue Sun. Frequency separation control for drag-free satellite with frequency-domain constraints. *IEEE Transactions on Aerospace and Electronic Systems*, 57(6):4085–4096, November 2021.
- [279] Zhijie Ma and Jihe Wang. A controller design method for drag-free spacecraft multiple loops with frequency domain constraints. *IEEE Transactions on Aerospace and Electronic Systems*, 59(3):3224–3235, November 2023.
- [280] Jikun Yang, Jinxiu Zhang, Jihe Wang, and Wenjian Tao. Kalman filter-based model predictive

- control for drag-free satellite under actuator failures and input saturations. *Review of Scientific Instruments*, 94(3):034502, March 2023.
- [281] Chunyu Xiao, Enrico Canuto, Wei Hong, Zebing Zhou, and Jun Luo. Drag-free design based on embedded model control for tianqin project. *Acta Astronautica*, 198:482–494, June 2022.
- [282] Menghao Zhao, Wei Hong, Chunyu Xiao, Yun Ma, Yanzheng Bai, and Zebing Zhou. High-precision ground simulator for laser tracking of gravity satellite. *Review of Scientific Instruments*, 95(2):024503, February 2024.
- [283] Weitong Fan, Chunzhao Ma, Danqing Liu, Rong Zhu, Guobin Zhou, Xuezhen Gong, Shungao Zhou, Jie Xu, Wenhao Yuan, Changlei Guo, and Hsien-Chi Yeh. Dual-frequency fundamental-mode npro laser for low-noise microwave generation. *OPTICS EXPRESS*, 31(8):13402–13413, APR 10 2023.
- [284] Guobin Zhou, Rong Zhu, Chunzhao Ma, Xuezhen Gong, Weitong Fan, Shungao Zhou, Jie Xu, Changlei Guo, and Hsien-chi Yeh. Unidirectional operation criterion in monolithic nonplanar ring oscillators. *OPTICS LETTERS*, 48(11):3047–3050, JUN 1 2023.
- [285] Jue Li, Weitong Fan, Jie Xu, Zelong Huang, Jian Luo, Xin Yu, Yunqiao Hu, Qisen Yang, Changlei Guo, and Hsien-Chi Yeh. Low-noise high-power dual-frequency mopa laser with an npro seed. *Opt. Express*, 33(3):4889–4901, Feb 2025.
- [286] Yingxin Luo, Hongyin Li, Yi-Qi Li, Zhen-Hai Zhan, Cheng-Ye Huang, Jin-Tao Lai, and Hsien-Chi Yeh. Prototype of a monolithic cavity-based ultrastable optical reference for space applications. *APPLIED OPTICS*, 60(10):2877–2885, APR 1 2021.
- [287] Zhenhai Zhan, Yingxin Luo, Hsien-Chi Yeh, Hongyin Li, Weilu Chen, Chongzhi Ren, and Bingcheng Zeng. Development of a space-compatible packaging system for an integrated monolithic ultra-stable optical reference. *Review of Scientific Instruments*, 95(10):104505, 10 2024.
- [288] G. Heinzel, C. Braxmaier, R. Schilling, A. Rüdiger, D. Robertson, M. te Plate, V. Wand, K. Arai, U. Johann, and K. Danzmann. Interferometry for the LISA technology package (LTP) aboard SMART-2. *Class. Quant. Grav.*, 20:S153–S161, 2003.
- [289] G. Heinzel et al. Successful testing of the LISA Technology Package (LTP) interferometer engineering model. *Class. Quant. Grav.*, 22:S149–S154, 2005.
- [290] Marina Dehne, Michael Troebs, Gerhard Heinzel, and Karsten Danzmann. Verification of polarising optics for the lisa optical bench. *OPTICS EXPRESS*, 20(25):27273–27287, DEC 3 2012.
- [291] M. Armano et al. Sensor Noise in *LISA Pathfinder* : In-Flight Performance of the Optical Test Mass Readout. *Phys. Rev. Lett.*, 126(13):131103, 2021.
- [292] M. Armano et al. Sensor noise in LISA Pathfinder: An extensive in-flight review of the angular and longitudinal interferometric measurement system. *Phys. Rev. D*, 106(8):082001, 2022.
- [293] Min Ming et al. Long-term stability of the picometer-resolution interferometer on TianQin-1 satellite. *Class. Quant. Grav.*, 41(16):165014, 2024.
- [294] Bin Cao, Fu-Ling Jia, Ming-Lin Yang, Fang-Jie Liao, Kai-Hang Wu, Xiang-Qing Huang, Min Ming, Jing-Yi Zhang, Shi-Zhe Wen, Hui-Zong Duan, and Hsien-Chi Yeh. Suppression of frequency-mixing effect for pm-level heterodyne interferometers based on “zero coupling” optical path length control. *OPTICS LETTERS*, 49(12):3300–3303, JUN 15 2024.
- [295] Oliver Gerberding, Christian Diekmann, Joachim Kullmann, Michael Troebs, Ioury Bykov, Simon Barke, Nils Christopher Brause, Juan Jose Esteban Delgado, Thomas S. Schwarze, Jens Reiche, Karsten Danzmann, Torben Rasmussen, Torben Vendt Hansen, Anders Enggaard, Soren Moller Pedersen, Oliver Jennrich, Martin Suess, Zoran Sodnik, and Gerhard Heinzel. Readout for intersatellite laser interferometry: Measuring low frequency phase fluctuations of high-frequency signals with microradian precision. *REVIEW OF SCIENTIFIC INSTRUMENTS*, 86(7), JUL 2015.
- [296] Yu-Rong Liang, Yu-Jie Feng, Guo-Yao Xiao, Yuan-Ze Jiang, Lin Li, and Xue-Lin Jin. Experimental scheme and noise analysis of weak-light phase locked loop for large-scale intersatellite laser interferometer. *REVIEW OF SCIENTIFIC INSTRUMENTS*, 92(12), DEC 1 2021.
- [297] Vinzenz Wand. *Interferometry at low Frequencies: Optical Phase Measurement for LISA and LISA Pathfinder*. PhD thesis, Hannover U., 5 2007.
- [298] Yu-Jie Feng, Yuan-Ze Jiang, Guo-Yao Xiao, Liu-Yang Chen, Bai-Fu Lu, Zhi-Lin Xu, and Yu-Rong Liang. Utilizing multi-point temperature sensing to evaluate the low frequency noise of phasemeter for intersatellite laser interferometer. *REVIEW OF SCIENTIFIC INSTRUMENTS*, 95(10), OCT 1 2024.
- [299] Wen Tong Fan, Jie Song, Hong Wen Hai, Si Jun Fang, Kai Zhao, Rui Zhang, Bo Hong Li, Jian Luo, Qi Cheng Sun, Lei Fan, Zi Zheng Li, Hsien-Chi Yeh, and Yong Yan. Research on

- the tilt-to-length coupling noise suppression method inside the gravitational wave detection telescope. *Opt. Express*, 32(7):12200–12212, Mar 2024.
- [300] Wentong Fan et al. The impact of telescope aberrations on the magnitude of tilt to length coupling noise in space based gravitational wave detectors. *Class. Quant. Grav.*, 40(24):245007, 2023.
- [301] Wentong Fan et al. Effect of the focusing system on measurements in gravitational wave detection telescope. *Class. Quant. Grav.*, 41(1):015023, 2024.
- [302] Zhenning Luo, Yiping Wang, Xinxin Liu, and ZiZheng Li. Calculation methods for thermo-optic noise and nonequilibrium noise in the coatings of space gravitational wave detection telescope. *Phys. Rev. D*, 110(10):102001, 2024.
- [303] Hongwen Hai, Qicheng Sun, Kai Zhao, Rurui Zou, and Yong Yan. Design and Analysis of a Telescope Optical Path Length Stability Measurement Scheme (in Chinese). *Chinese Journal of Lasers*, 51(6):0604002, 2024.
- [304] HongWen Hai, Sijun Fang, WenTong Fan, QiCheng Sun, Kai Zhao, Rui Zhang, BoHong Li, Jian Luo, Jie Song, YeHao Cao, XinYu Li, ZiZheng Li, Lei Fan, HongChao Zhao, and Yong Yan. Analysis of alignment requirements for off-axis resonant cavity based on coupling efficiency. *Appl. Opt.*, 63(6):1488–1494, Feb 2024.